A Strain-Based Approach for Geometrically Nonlinear Aeroelasticity

Weihua Su

Department of Aerospace Engineering and Mechanics
University of Alabama
Tuscaloosa, AL

Presented at the School of Aeronautic Science and Engineering
Beijing University of Aeronautics and Astronautics
Beijing, China
July 29, 2013

About Me …

- Assistant Professor, University of Alabama
- Education
  - B.S. 2000 (BUAA)
  - M.S. 2002 (BUAA)
  - Ph.D. 2008 (Univ. of Michigan)
- Research areas
  - Nonlinear aeroelasticity
  - Structural dynamics
  - Active/smart structures
  - Flight dynamics
  - Active control
  - UAV, MAV, Wind Turbine, etc.

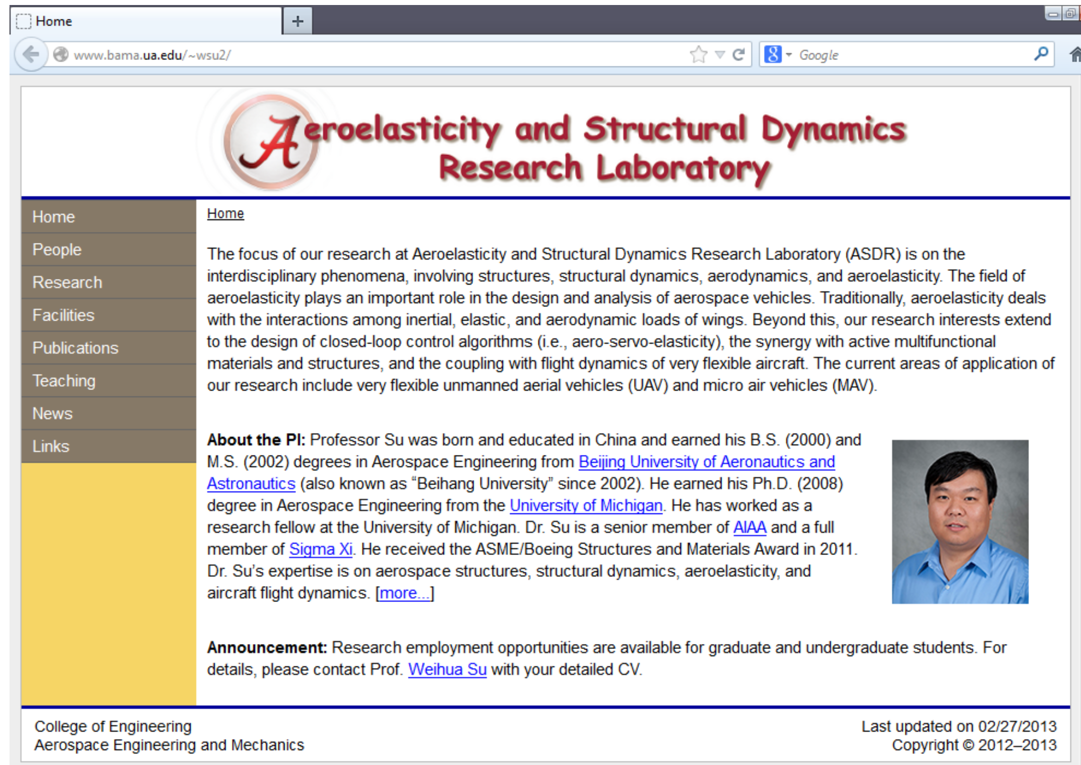

- Research lab:
  - Aeroelasticity and Structural Dynamics Research Laboratory
  - www.bama.ua.edu/~wsu2/

Overview

- Introduction
  - Motivation and background
  - Objective
- Nonlinear aeroelastic formulation
  - Geometrically nonlinear beam model
  - Aerodynamic and flight dynamic formulations
- Numerical studies
  - Flutter instability
  - Response to external disturbance (gust)
- UAV design and flight tests
- Concluding remarks
- Other research areas

High-Altitude Long-Endurance (HALE) Aircraft

- Aircraft for surveillance, target acquisition, and communications
- Desired features:
  - long operation range
  - long loiter time

$$R \text{ or } E \propto \left(\frac{L}{D}\right) \ln\left(\frac{W_0}{W_1}\right)$$

High aerodynamic efficiency

Low structural weight fraction

+

High-aspect-ratio wings

Very flexible aircraft

Wing Aspect Ratio and Aerodynamic Efficiency

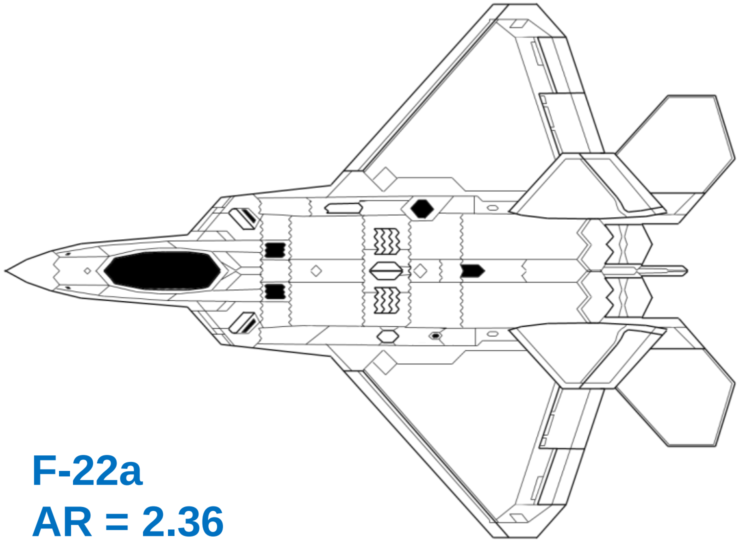

F-22a
AR = 2.36

B787-8
AR = 11.08

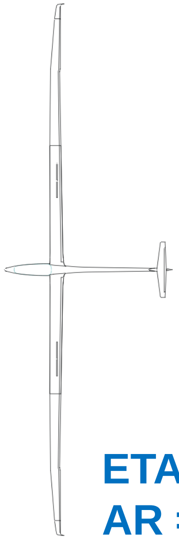

ETA (Germany)
AR = 51.33

Large aspect ratio for high aerodynamic efficiency

But…The large AR brings something interesting

U.S. Air Force Sensorcraft Studies

- HALE aircraft may adopt rather unconventional configurations:
- Unmanned vehicles
- Sensor platform
- Very high fuel fractions (up to 60%)

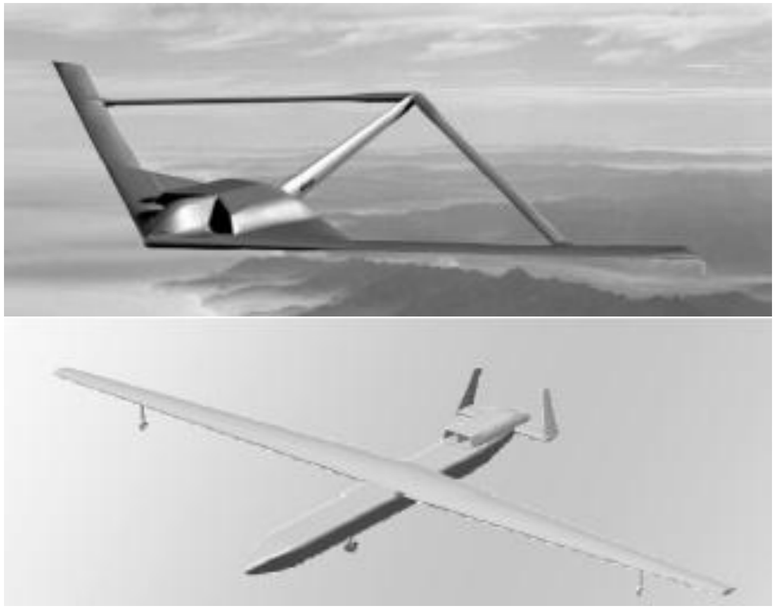

ISR (intelligence, surveillance, reconnaissance)
“Sensorcraft” Concepts (Lucia, 2005)

Pushing the Flight Envelop…

AeroVironment's Helios: >24 hrs

AeroVironment's Global Observer: One week

DARPA's Vulture Program: >5 years

High lift-to-drag ratio wings and low structural weight fraction

Background

- Aeroelastic response of vehicles with long, high-aspect-ratio wings is inherently nonlinear:
  - Large elastic deflections: structurally nonlinear
  - Large angles of attack: aerodynamic nonlinear
  - Local transonic effects: aerodynamic nonlinear
- Low frequency aeroelastic response couples with flight dynamics with nonlinearities possibly dominating the vehicle response
  - Trajectory and attitude
  - Stability (including body-freedom flutter)
  - Response to disturbances
- Combined nonlinear effects alter loads, stability, performance

Mishap of Helios Prototype

The number one root cause/recommendation from NASA[1] was:

[That] more advanced, multidisciplinary (structures, aeroelastic, aerodynamics, atmospheric, materials, propulsion, controls, etc.) time-domain analysis methods appropriate to highly flexible, morphing vehicles [be developed].

[1] Noll, T. E., Brown, J. M., Perez-Davis, M. E., Ishmael, S. D., Tiffany, G. C., and Gaier, M., “Investigation of the Helios Prototype Aircraft Mishap,” Tech. rep., NASA, January 2004.

Focus

- Objective:
  - Understand the aeroelastic response of very flexible aircraft during normal and unusual flight conditions
    - Structural integrity
    - Stability
    - Controllability
  - Generate parametric models for concept design of unconventional configurations
  - Explore different electric/mechanical/aero mechanisms for vehicle aeroelastic control
- Approach:
  - Develop reduced-order aeroservoelastic formulation
    - For preliminary vehicle and control design studies or more detailed analysis
    - Able to simulate fully flexible vehicle with 6 rigid-body DoF's
  - Numerically investigate aeroelastic response of different vehicle configurations under different nonlinear effects

Reduced-Order Aeroelastic Framework

A Multidisciplinary Approach

Incompressible 2-D unsteady aerodynamics, Prandtl-Glauert and tip loss corrections, stall model

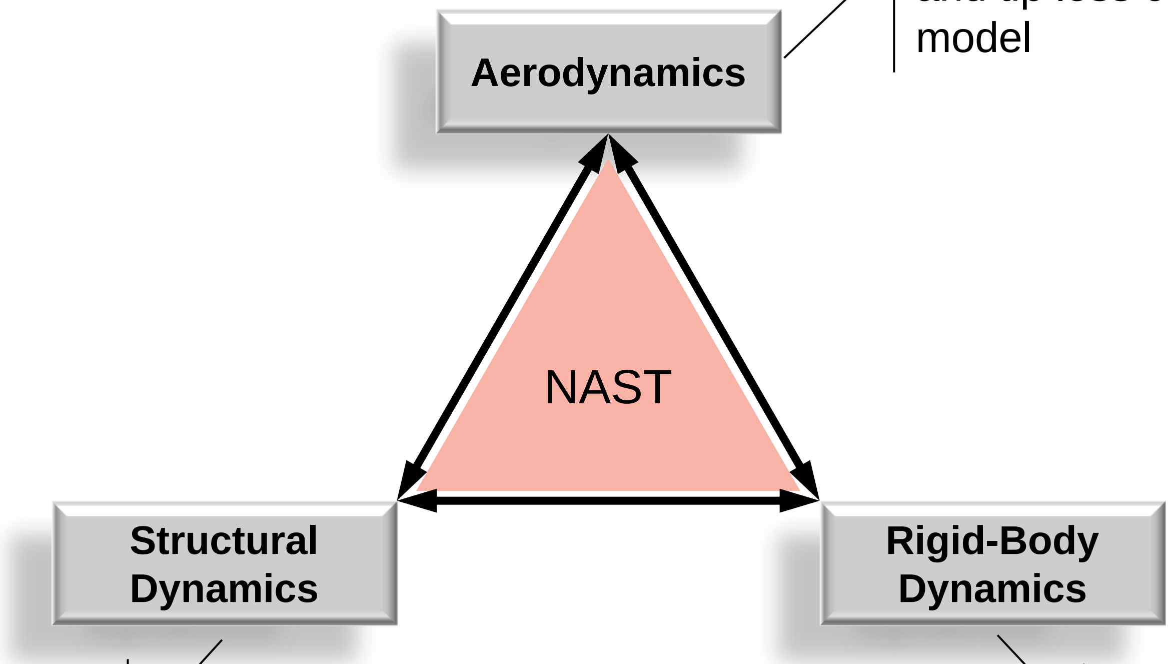

Strain-based geometrically nonlinear composite beam

Nonlinear 6-DoF vehicle dynamics

Simplified free-flight analysis and simulation for full aircraft

Reduced-Order Aeroelastic Framework (Cont'd)

A Multidisciplinary Approach

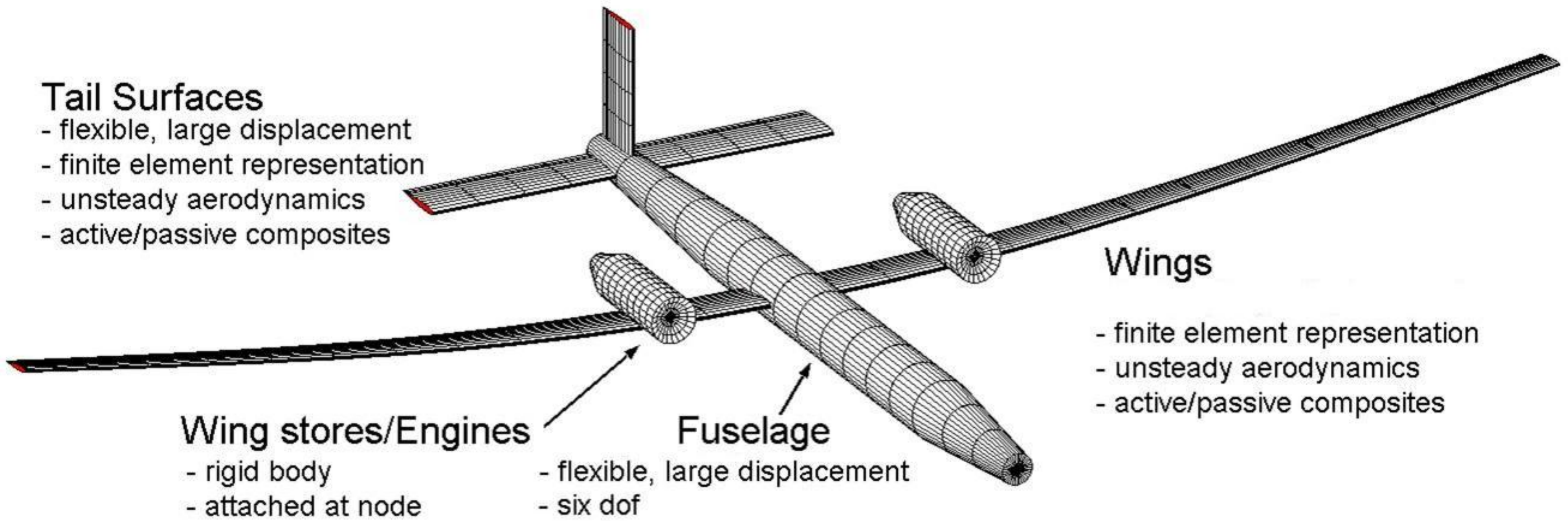

Simplified free-flight analysis and simulation for full aircraft

Reduced-Order Structural Modeling

- From 3D elastic problem to 2D beam cross-sectional analysis and 1D beam model
- Dimensional reduction using the Variational-Asymptotic Method:
  - Active thin-walled solution (mid-line discretization)
  - VABS (finite-element discretization)
  - User defined stiffness constants

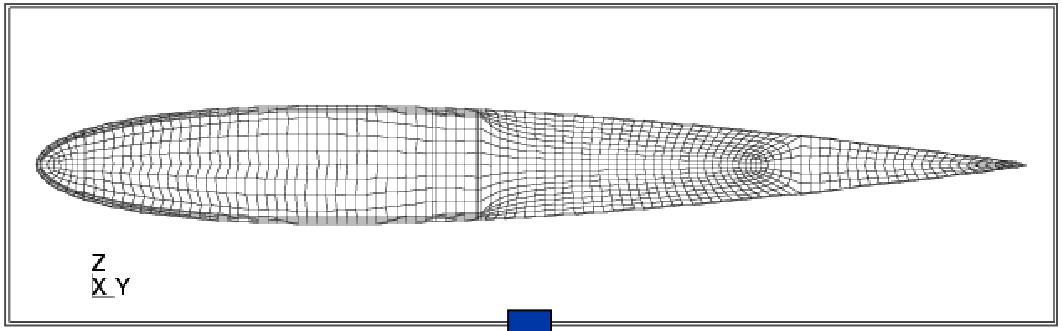

Cross-Section Stiffness and Actuation Constants

$$\begin{bmatrix} F_x \\ M_x \\ M_y \\ M_z \end{bmatrix} = \begin{bmatrix} K_{11} & K_{12} & K_{13} & K_{14} \\ K_{21} & K_{22} & K_{23} & K_{24} \\ K_{31} & K_{32} & K_{33} & K_{34} \\ K_{41} & K_{42} & K_{43} & K_{44} \end{bmatrix} \begin{bmatrix} \varepsilon_x \\ \kappa_x \\ \kappa_y \\ \kappa_z \end{bmatrix} - \begin{bmatrix} B_{11} & B_{12} & \cdots & B_{1m} \\ B_{21} & B_{22} & \cdots & B_{2m} \\ B_{31} & B_{32} & \cdots & B_{3m} \\ B_{41} & B_{42} & \cdots & B_{4m} \end{bmatrix} \begin{bmatrix} v_1 \\ v_2 \\ \vdots \\ v_m \end{bmatrix}$$

Highlight of Strain-Based Geometrically Nonlinear Beam Formulation

- Geometrically exact formulation – no approximation to deformation of beam reference line
- Reduced number of degrees of freedom
- Efficient in solving geometrically nonlinear static problem
- Beam strain (curvature) is directly measured by control sensor – facilitate control design and study
- Catch geometrically nonlinear behavior of flexible isotropic and composite wings
- Provide structural dynamic models for nonlinear aeroelastic and control studies of very flexible slender structures

- Difficulty in solving statically indeterminate beams – with splits and joints

Basic Coordinate Systems

- Global frame (G)
- Body frame (B) – origin not necessary to be C.G. of vehicle
- Body frame motion variables

$$b = \begin{Bmatrix} p_B \\ \theta_B \end{Bmatrix}$$

$$\dot{b} = \beta = \begin{Bmatrix} \dot{p}_B \\ \dot{\theta}_B \end{Bmatrix} = \begin{Bmatrix} v_B \\ \omega_B \end{Bmatrix}$$

$$\ddot{b} = \dot{\beta} = \begin{Bmatrix} \ddot{p}_B \\ \ddot{\theta}_B \end{Bmatrix} = \begin{Bmatrix} \dot{v}_B \\ \dot{\omega}_B \end{Bmatrix}$$

- Local beam frame (w)
- Auxiliary local frame (b)

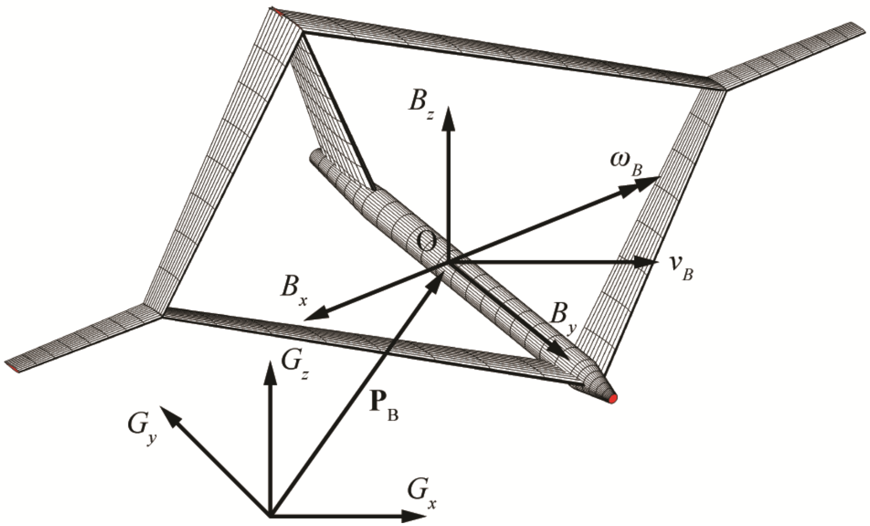

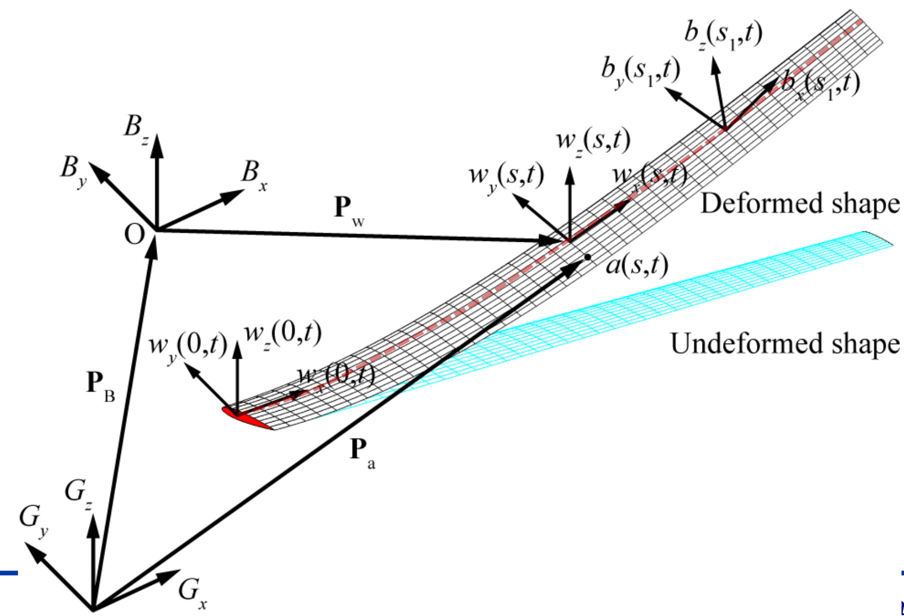

Strained-Based Finite Element Beam Formulation

- Geometrically nonlinear beam formulation[2]
- Four local strain degrees-of-freedom (ε): extension, twist, flatwise bending, and chordwise bending
- Constant-strain elements
- Capture large complex deformations with fewer elements – computationally efficient
- Isotropic and anisotropic constitutive relations

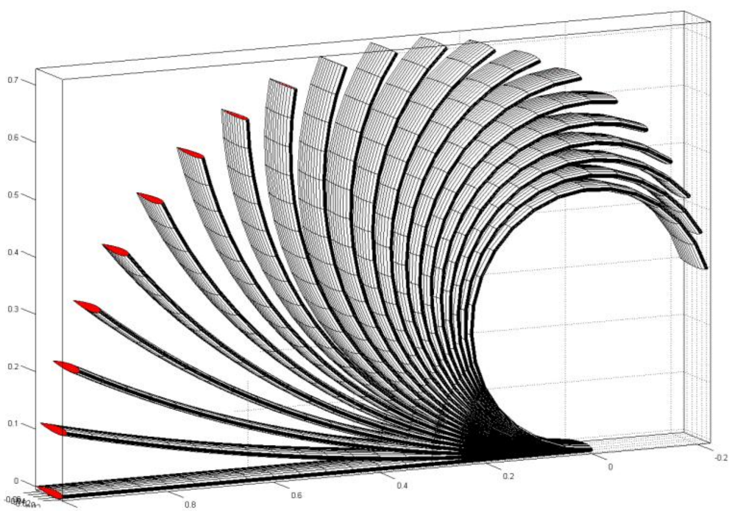

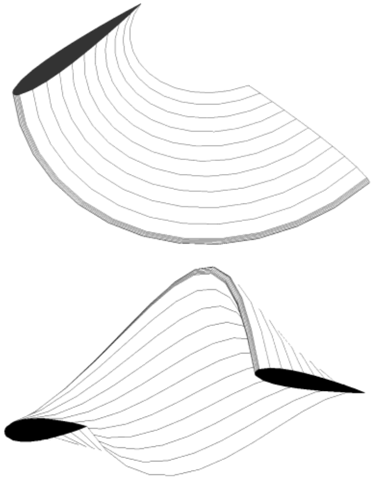

Sample element deformations with constant strain

Strains (ε) and body velocities (β) are independent variables

[2] Su, W., and Cesnik, C. E. S., "Strain-Based Geometrically Nonlinear Beam Formulation for Modeling Very Flexible Aircraft," *International Journal of Solids and Structures*, Vol. 48, No. 16-17, 2011, pp. 2349-2360. doi: 10.1016/j.ijsolstr.2011.04.012

Nodal Position and Orientation

- Arbitrary point in a cross-section (a)

$$\mathbf{p}_a = \underline{\mathbf{p}_B} + \underline{\mathbf{p}_w + x\mathbf{w}_x + y\mathbf{w}_y + z\mathbf{w}_z}$$

Body Frame Motion **Elastic Strain Contribution**

- Position and orientation of nodes along beam reference line

$$h^T(s) = \left\{\mathbf{p}_B^T + \mathbf{p}_w^T(s), \quad \mathbf{w}_x^T(s), \quad \mathbf{w}_y^T(s), \quad \mathbf{w}_z^T(s)\right\}$$

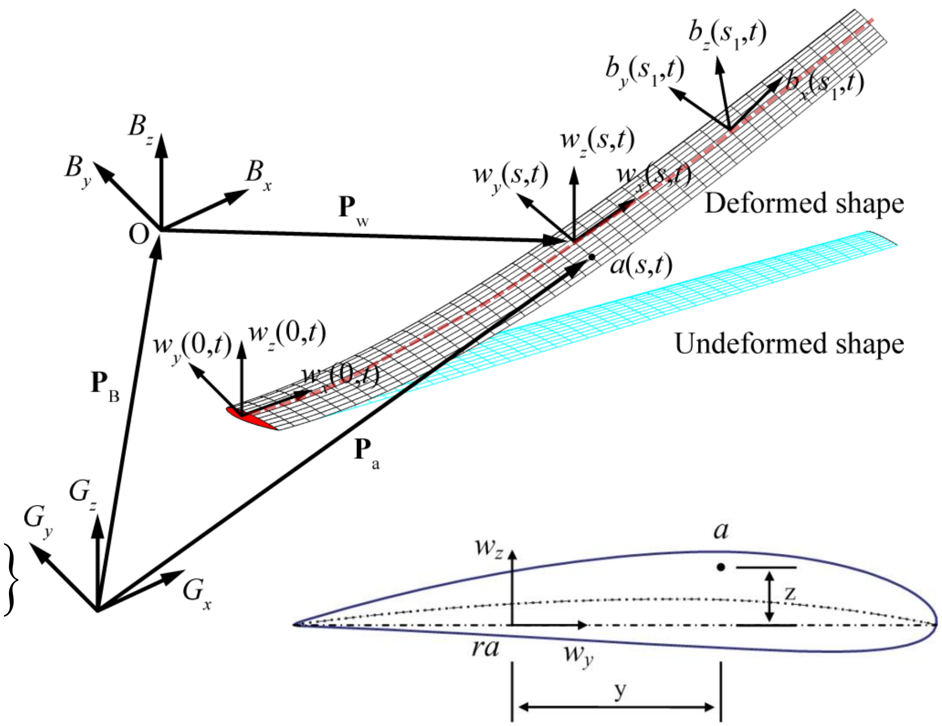

- Differential and variation of h are related to ε and β

$$\delta h = J_{h\varepsilon}\delta\varepsilon + J_{hb}\delta b$$

$$dh = J_{h\varepsilon}d\varepsilon + J_{hb}db$$

$$\dot{h} = J_{h\varepsilon}\dot{\varepsilon} + J_{hb}\dot{b} = J_{h\varepsilon}\dot{\varepsilon} + J_{hb}\beta$$

$$\ddot{h} = J_{h\varepsilon}\ddot{\varepsilon} + \dot{J}_{h\varepsilon}\dot{\varepsilon} + J_{hb}\dot{\beta} + \dot{J}_{hb}\beta$$

where $J_{h\varepsilon} = \dfrac{\partial h}{\partial \varepsilon}$, $J_{hb} = \dfrac{\partial h}{\partial b}$

Virtual Work – Inertia of Flexible Beam Members

- Inertia force

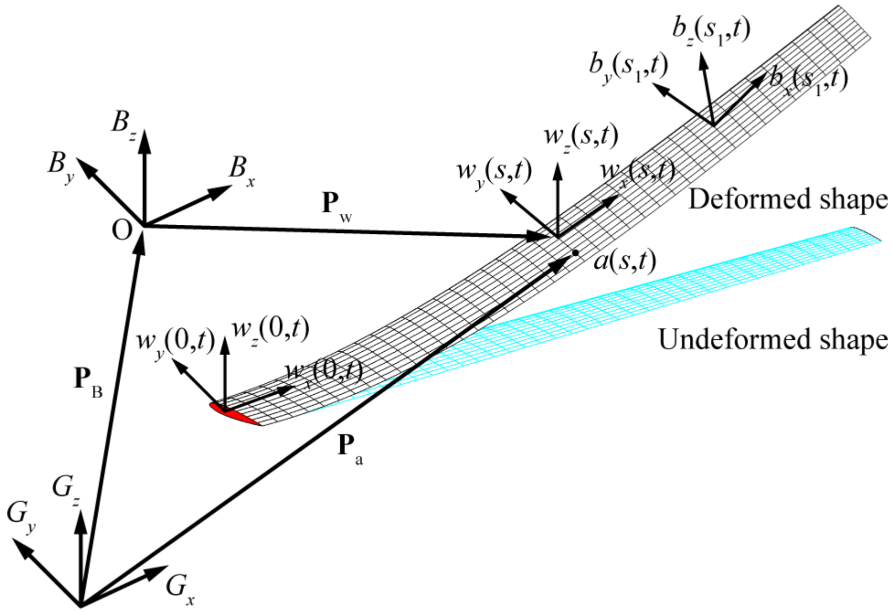

Position: $\mathbf{p}_a$

↓

Velocity and acceleration:

$\mathbf{v}_a$, $\mathbf{a}_a$

↓

Virtual work:

$$\delta W^{int} = \int_V \delta \mathbf{p}_a \cdot \left(-\mathbf{a}_a \rho dAds \right)$$

- Consists of virtual displacement δh and dependent variable $\ddot{h}$

Virtual Work of Flexible Beam Members

- Internal strain and strain rate

$$\delta W^{int} = \int_s \left[-\delta\varepsilon(s)^T k(s)\left(\varepsilon(s) - \varepsilon^0(s)\right) - \delta\varepsilon(s)^T c(s)\dot{\varepsilon}(s) \right] ds$$

- Virtual work of external load

$$\delta W^{ext} = \int_V \delta u^T(x,y,z) f(x,y,z) dV$$

- Assembly of total virtual work

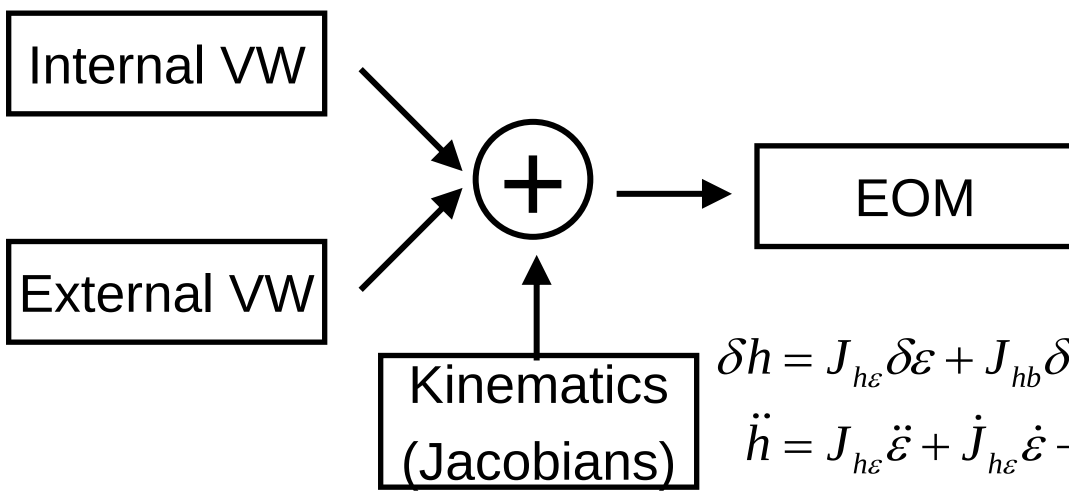

Strain-based form

$$\delta h = J_{h\varepsilon}\delta\varepsilon + J_{hb}\delta b$$

$$\ddot{h} = J_{h\varepsilon}\ddot{\varepsilon} + \dot{J}_{h\varepsilon}\dot{\varepsilon} + J_{hb}\dot{\beta} + \dot{J}_{hb}\beta$$

$$\cdots$$

Formulation Based on Principle of Virtual Work

$$\sum_i \delta W_i = 0$$

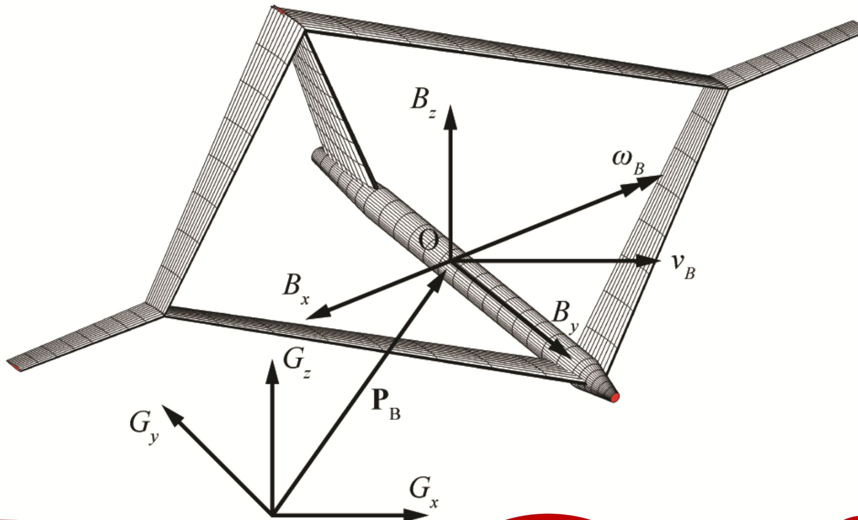

Equations of Motion

$$\begin{bmatrix} M_{FF}(\varepsilon) & M_{FB}(\varepsilon) \\ M_{BF}(\varepsilon) & M_{BB}(\varepsilon) \end{bmatrix} \begin{Bmatrix} \ddot{\varepsilon} \\ \dot{\beta} \end{Bmatrix} + \begin{bmatrix} C_{FF}(\varepsilon,\dot{\varepsilon},\beta) & C_{FB}(\varepsilon,\dot{\varepsilon},\beta) \\ C_{BF}(\varepsilon,\dot{\varepsilon},\beta) & C_{BB}(\varepsilon,\dot{\varepsilon},\beta) \end{bmatrix} \begin{Bmatrix} \dot{\varepsilon} \\ \beta \end{Bmatrix} + \begin{bmatrix} K_{FF} & 0 \\ 0 & 0 \end{bmatrix} \begin{Bmatrix} \varepsilon \\ b \end{Bmatrix} = \begin{Bmatrix} R_F \\ R_B \end{Bmatrix}$$

Generalized Mass **Generalized Damping** **Generalized Stiffness** **Generalized Force**

$$\begin{Bmatrix} R_F \\ R_B \end{Bmatrix} = \begin{Bmatrix} K_{FF}\varepsilon^0 \\ 0 \end{Bmatrix} - \begin{bmatrix} J_{h\varepsilon}^T \\ J_{hb}^T \end{bmatrix} Ng + \begin{bmatrix} J_{p\varepsilon}^T \\ J_{pb}^T \end{bmatrix} B^F F^{dist} + \begin{bmatrix} J_{\theta\varepsilon}^T \\ J_{\theta b}^T \end{bmatrix} B^M M^{dist} + \begin{bmatrix} J_{p\varepsilon}^T \\ J_{pb}^T \end{bmatrix} F^{pt} + \begin{bmatrix} J_{\theta\varepsilon}^T \\ J_{\theta b}^T \end{bmatrix} M^{pt}$$

Unsteady Aerodynamics – Finite-State Inflow Theory

- 2-D Theodorsen-like unsteady aerodynamics (Peters et al., 94, 95)

Inflow velocity

$$l_{mc} = \pi\rho_\infty b^2\left(-\ddot{z} + \dot{y}\dot{\alpha} - d\ddot{\alpha}\right) + 2\pi\rho_\infty b\dot{y}^2\left[-\frac{\dot{z}}{\dot{y}} + \left(\frac{1}{2}b - d\right)\frac{\dot{\alpha}}{\dot{y}} - \frac{\lambda_0}{\dot{y}}\right] + 2\pi\rho_\infty b c_1 \dot{y}^2\delta$$

$$m_{mc} = \pi\rho_\infty b^2\left(-\frac{1}{8}b^2\ddot{\alpha} - \dot{y}\dot{z} - d\dot{y}\dot{\alpha} - \dot{y}\lambda_0\right) + 2\pi\rho_\infty b^2 c_4 \dot{y}^2\delta$$

- Glauert expansion of inflow velocity as function of inflow states, λ_n

$$\lambda_0 = \frac{1}{2}\sum_{n=1}^{N} b_n\lambda_n$$

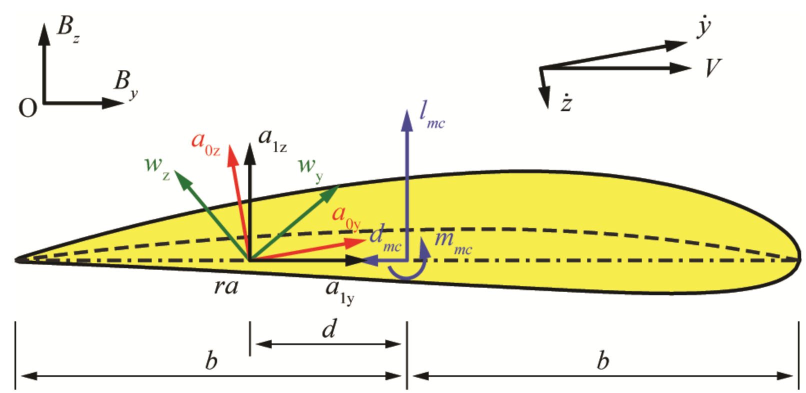

- Finite state differential equation is transformed to independent variables ε and β

$$\dot{\lambda} = E_1\lambda + E_2\ddot{z} + E_3\ddot{\alpha} + E_4\dot{\alpha} \quad \Rightarrow \quad \dot{\lambda} = F_1\begin{Bmatrix}\ddot{\varepsilon}\\ \dot{\beta}\end{Bmatrix} + F_2\begin{Bmatrix}\dot{\varepsilon}\\ \beta\end{Bmatrix} + F_3\lambda$$

Finite-State Inflow Theory: Modifications

- Aerodynamic coefficient from XFoil (Re effects)
- Compressibility accounted for by Prandtl-Glauert correction
- Spanwise aerodynamic corrections

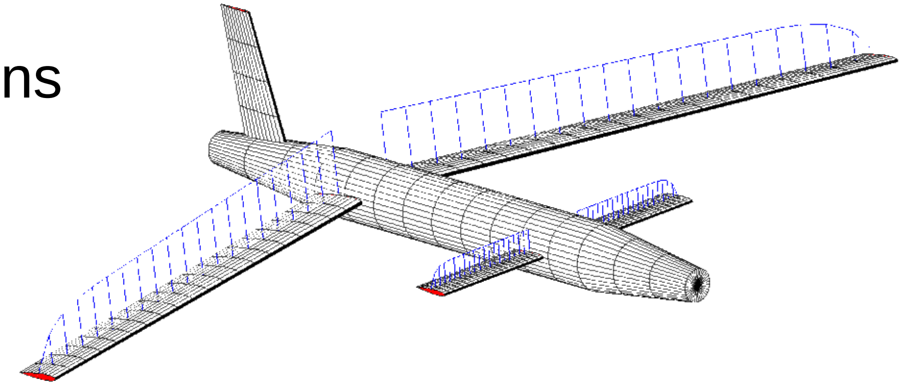

$$f_{Lcorr} = 1 - e^{-\tau s}$$

- Simplified stall model

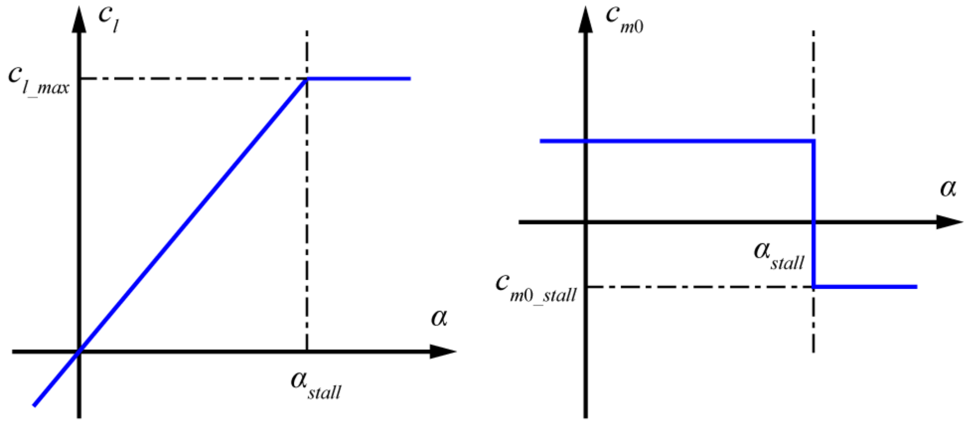

(a) Lift coefficient (b) Moment coefficient

Flight Dynamics Modeling

The trajectory and orientation of a fixed body reference frame, *B*, at point *O*, which in general is *not* the aircraft's center of mass

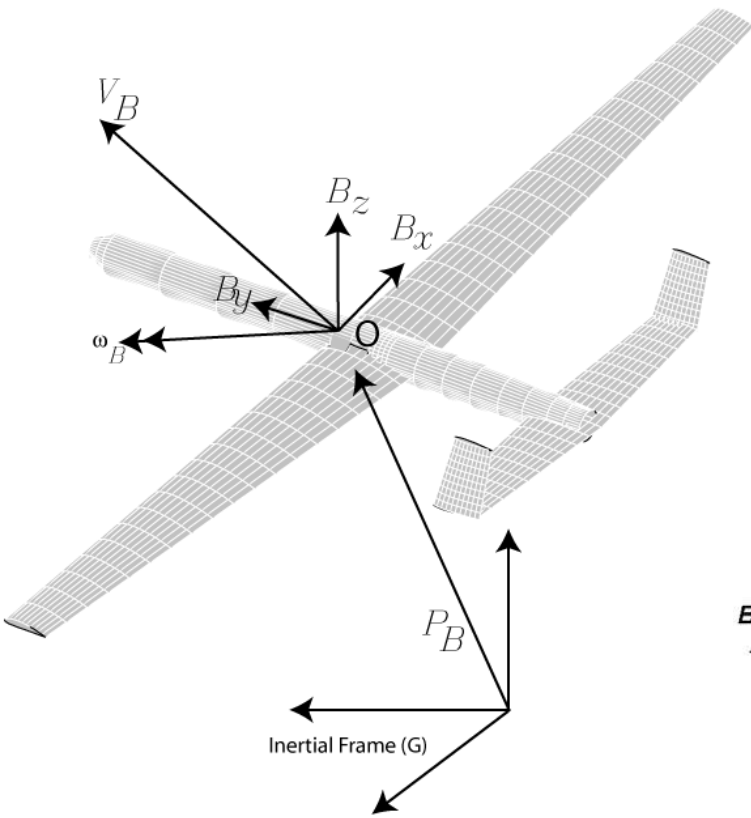

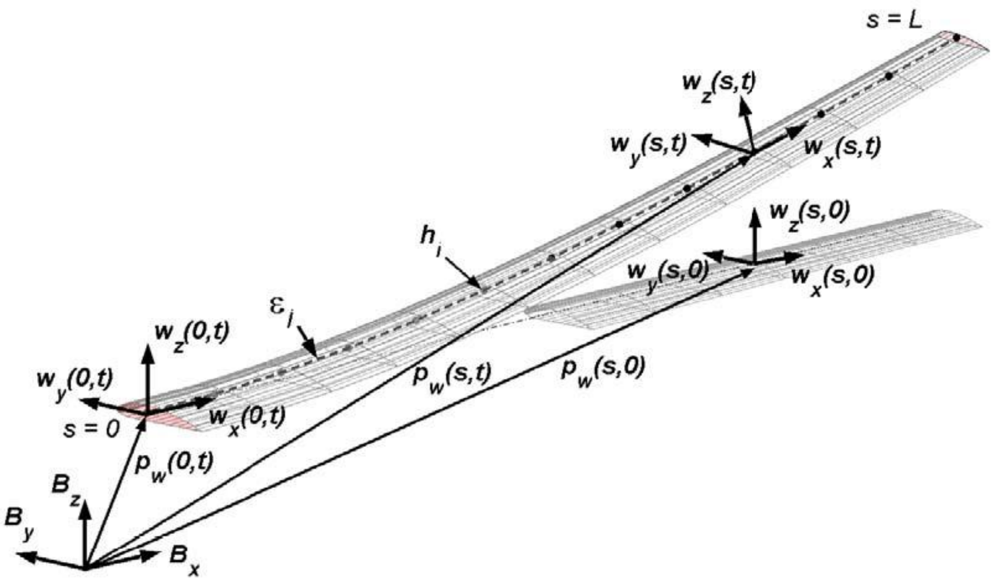

Complete-Aircraft Dynamics Model

- Elastic equations of motion

$$M(\varepsilon)\begin{Bmatrix}\ddot{\varepsilon}\\ \dot{\beta}\end{Bmatrix}+C(\varepsilon,\dot{\varepsilon},\beta)\begin{Bmatrix}\dot{\varepsilon}\\ \beta\end{Bmatrix}+K\begin{Bmatrix}\varepsilon\\ b\end{Bmatrix}=R(\varepsilon,\dot{\varepsilon},\ddot{\varepsilon},p_B,\zeta,\beta,\dot{\beta},\lambda,u)$$

Strains (4 by N structural d.o.f.)

Control inputs

Body velocities (6 flight dynamic d.o.f.)

- Finite-state 2-D unsteady aerodynamics

$$\dot{\lambda}=F_1\begin{Bmatrix}\ddot{\varepsilon}\\ \dot{\beta}\end{Bmatrix}+F_2\begin{Bmatrix}\dot{\varepsilon}\\ \beta\end{Bmatrix}+F_3\lambda$$

Inflow states (m by N aerodynamic d.o.f.)

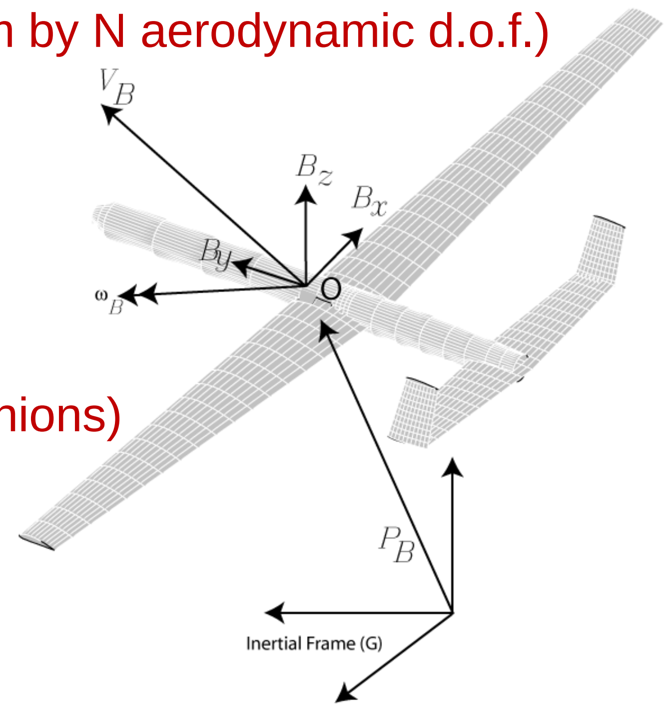

- Body reference frame propagation

$$\dot{\zeta}=-\frac{1}{2}\Omega_\zeta\zeta$$

Frame orientation (4 quaternions)

$$\dot{P}_B=\begin{bmatrix}C^{GB} & 0\end{bmatrix}\beta$$

Inertial velocities (6 d.o.f.)

NAST: Function Block Diagram

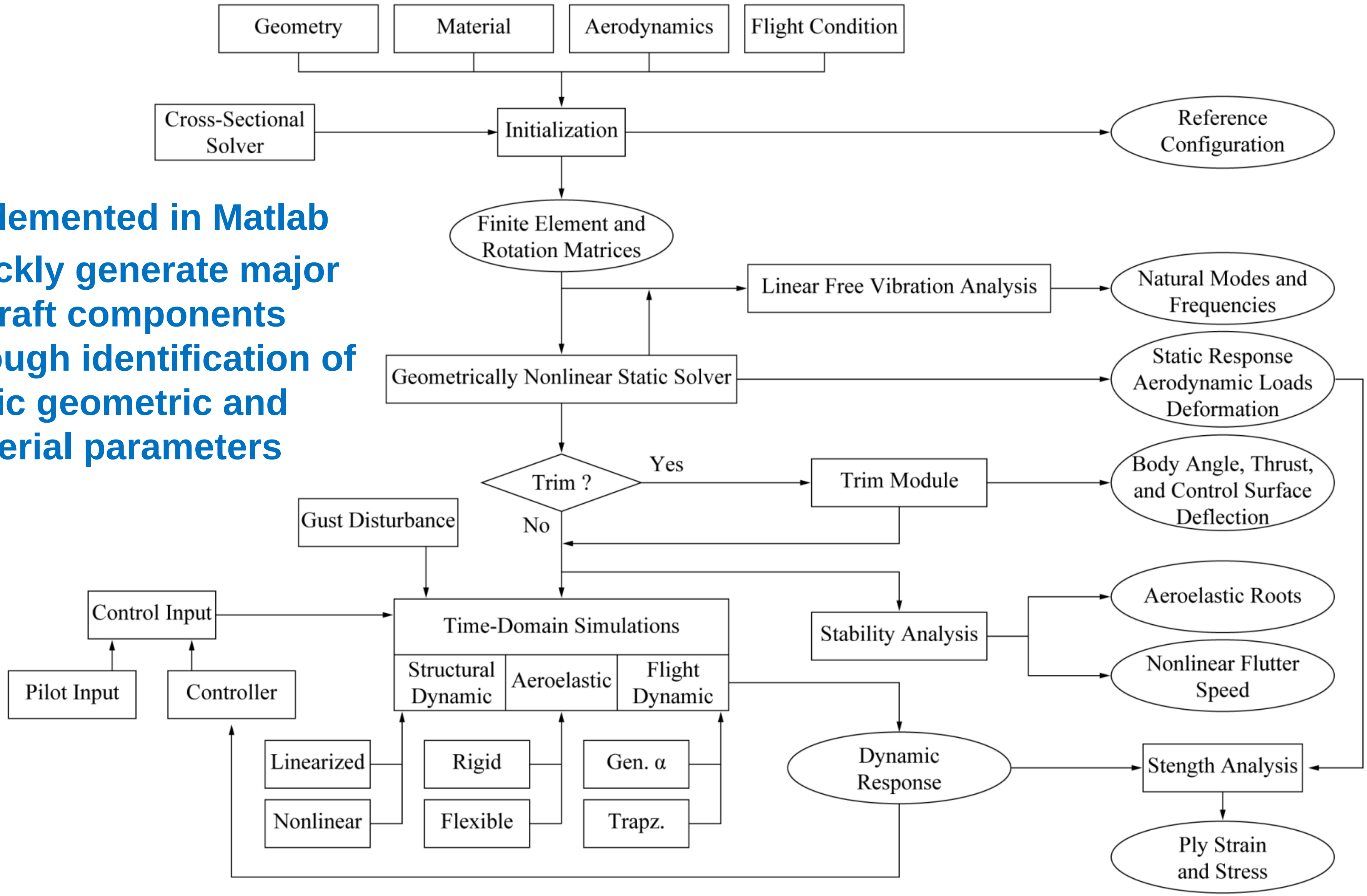

Implemented in Matlab

Quickly generate major aircraft components through identification of basic geometric and material parameters

Nonlinear Aeroelastic Simulation Toolbox (NAST)

NAST is implemented in Matlab

Automatic generation of major aircraft components through identification of basic geometric and material parameters

<u>Solutions</u>:

- Nonlinear aeroelastic steady state deformation/trim solution
- Linearized aeroelastic response
- Fully nonlinear time-marching aeroelastic simulation
- Recovery of ply stress/strain, evaluation of ply failure
- Evaluation of flutter instability boundary, LCO
- Simulation of free flight of fully flexible vehicle
- Structure and aeroelastic modes and frequencies
- Closed-loop aeroelastic simulation

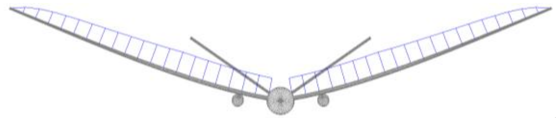

steady aerodynamic solution

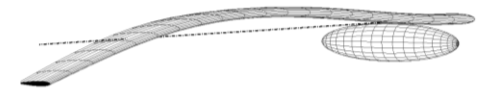

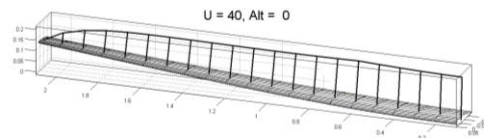

large structure deformation

failure analysis

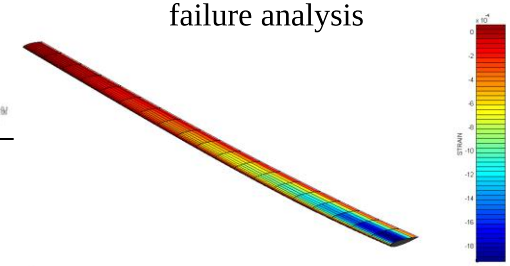

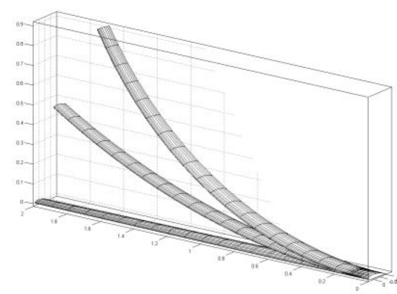

pre-twist and curvature

ply stress/strain distribution

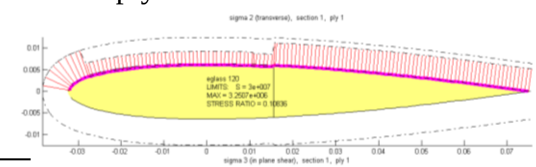

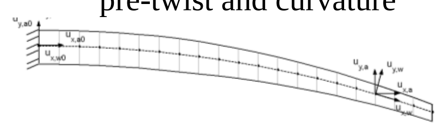

cross-section model

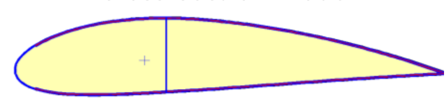

maneuver characteristics

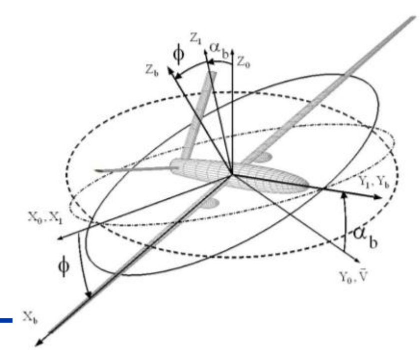

discrete control surfaces

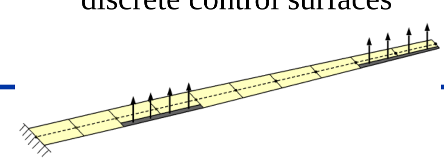

Numerical Studies

Blended-Wing-Body (BWB) Model

- Properties inspired from HiLDA (High Lift over Drag Active Wing) wind-tunnel model

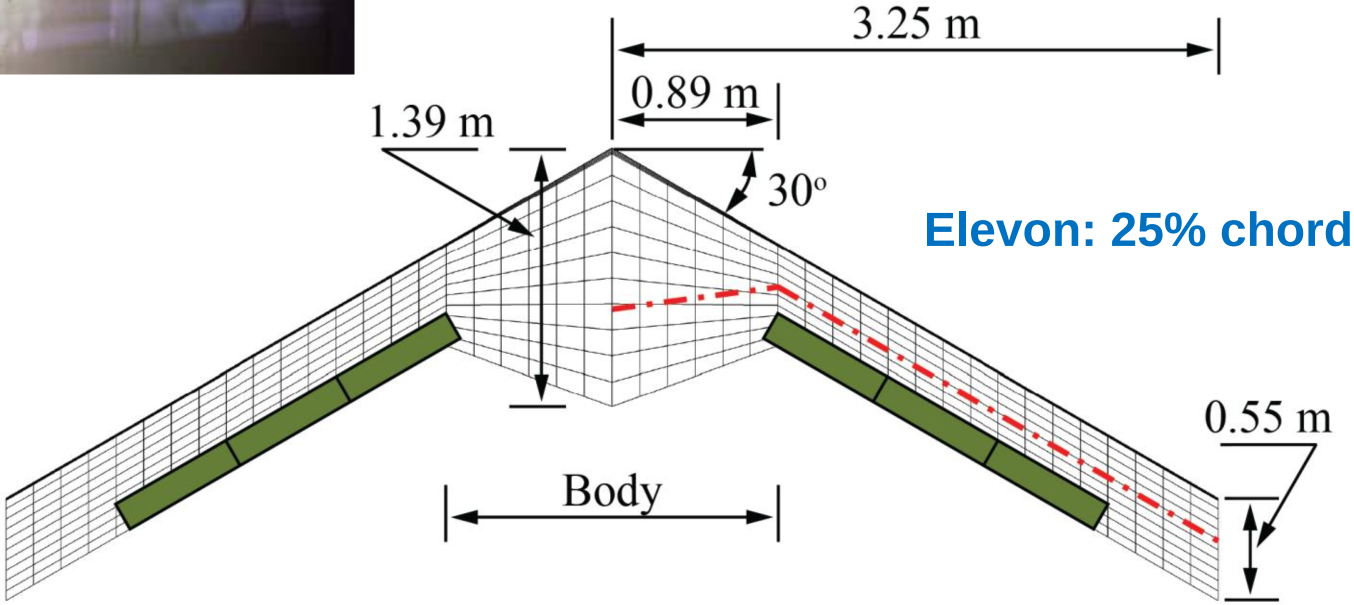

Elevon: 25% chord

Flutter of Constrained Vehicle

- Similar to constrained wind-tunnel model (no body DOFs)
- Fixed root angle of attack (8 deg)
- Free stream velocity 1% higher than flutter speed

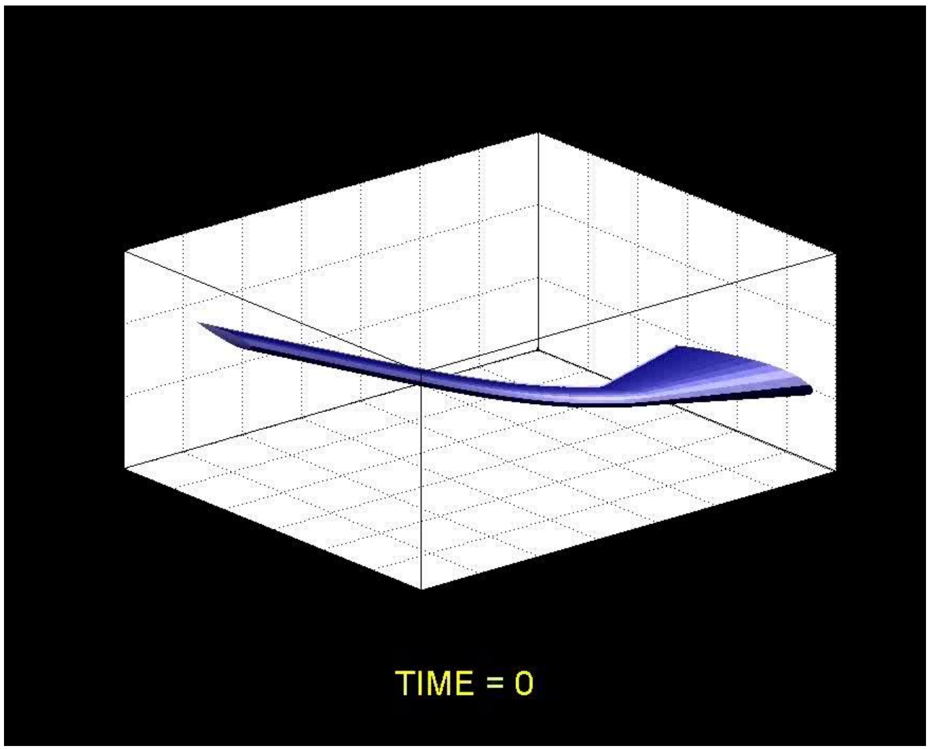

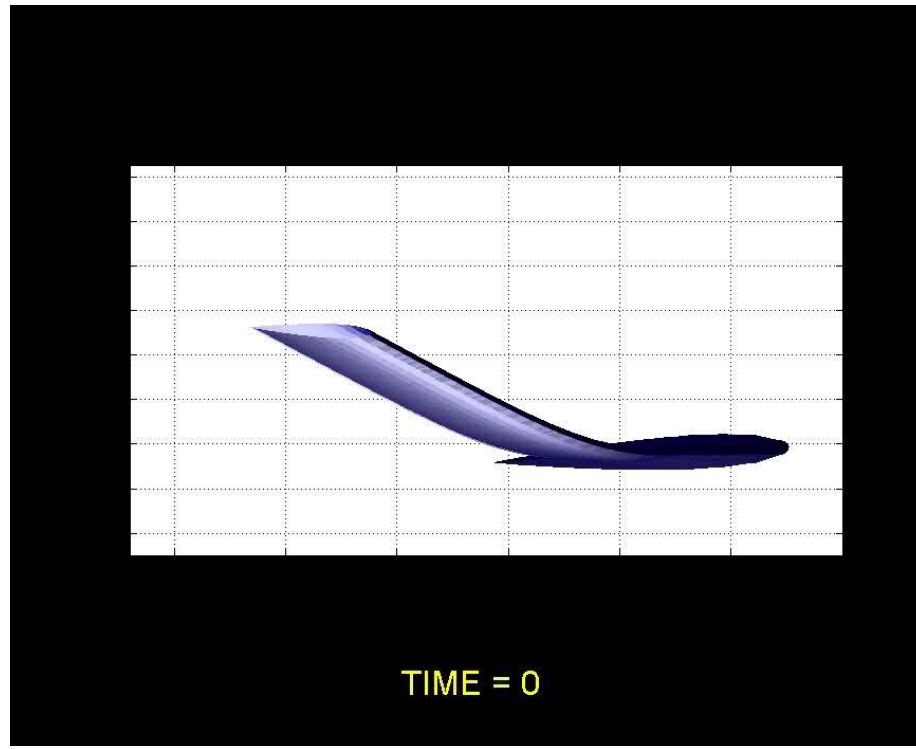

Coupled out-of-plane bending/torsion/in-plane bending mode

Comparison of Flutter Modes with Rigid-Body Constraints

All cases trimmed for 6,096 m (20,000 ft) altitude, same fuel condition

	Flutter Speed	Frequency
Fully constrained dof's	172.52 m/s	7.30 Hz
+ plunging	164.17 m/s	7.07 Hz
+ pitching and plunging	123.17 m/s	3.32 Hz
Free flight	123.20 m/s	3.32 Hz

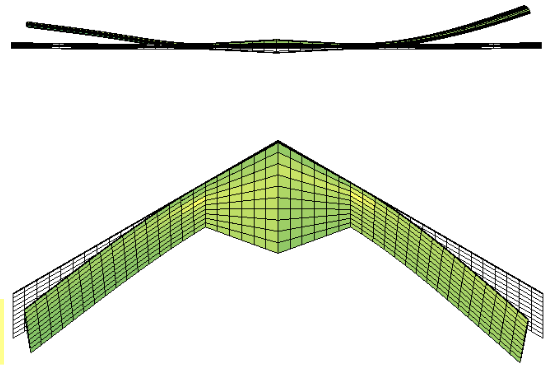

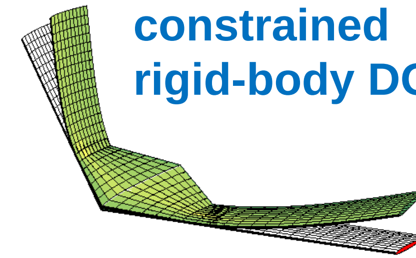

Fully constrained rigid-body DOFs

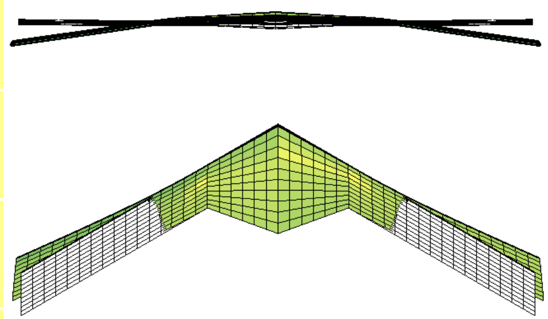

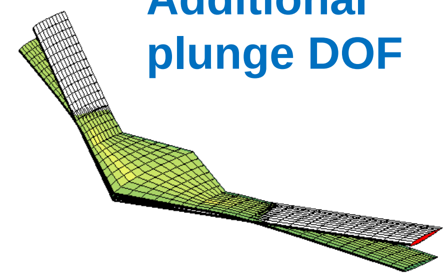

Additional plunge DOF

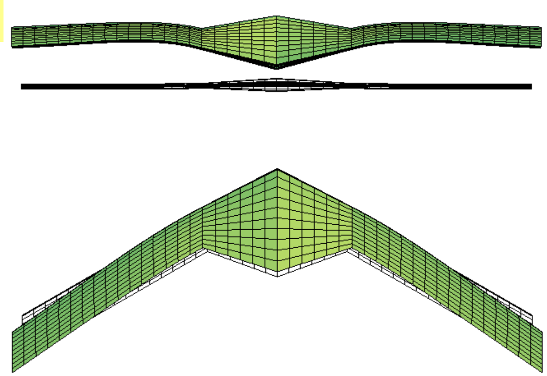

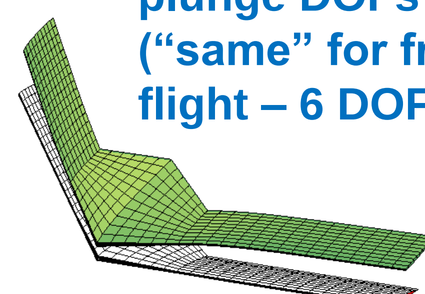

With pitch and plunge DOFs (“same” for free flight – 6 DOFs)

Traditional wind-tunnel setup maybe non-conservative – need rigid-body DOFs in the aeroelastic analyses, simulations, and tests

Highly Flexible Flying Wing Model

- Representative of Helios prototype[3]
  - Five engines and three pods
  - Payloads applied at center pod
  - Empty gross mass: 726 kg

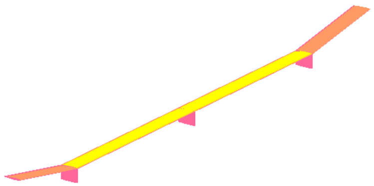

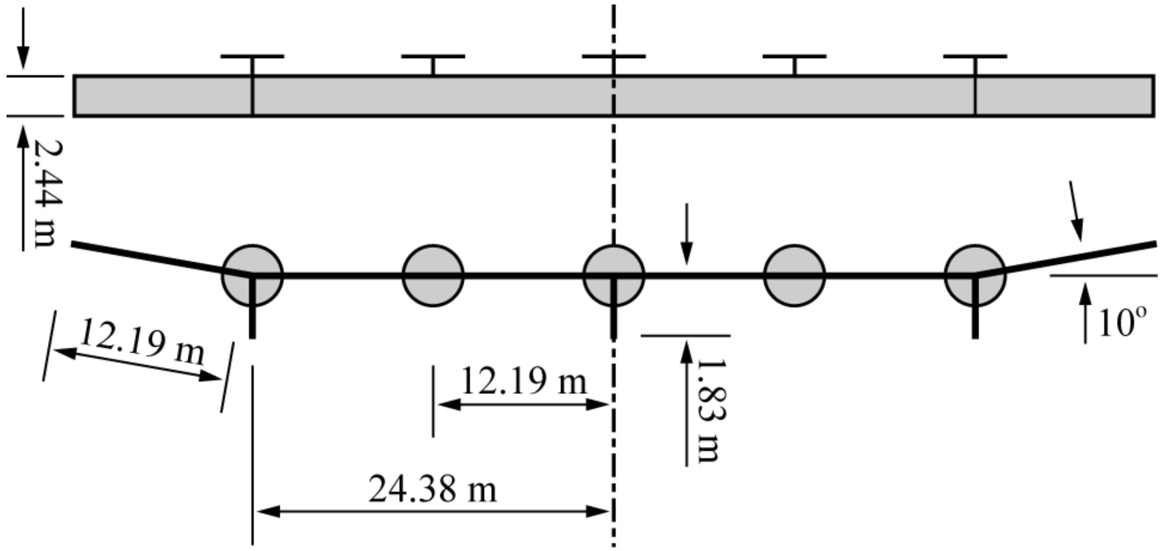

[3] Patil, M. J., and Hodges, D. H., "Flight Dynamics of Highly Flexible Flying Wings," *Journal of Aircraft*, Vol. 43, No. 6, 2006, pp. 1790-1798.

Trim Results and Flight Stability

- Speed: 12.2 m/s at sea level; Payload: 0 – 227 kg (at center pod)
- Linearization about each trimmed condition with increase of payloads
- Root locus for phugoid mode (left: flexible, right: rigid)
- Unstable phugoid mode for payload > 152 kg

Zero payload: span-loaded

Full payload: center-loaded

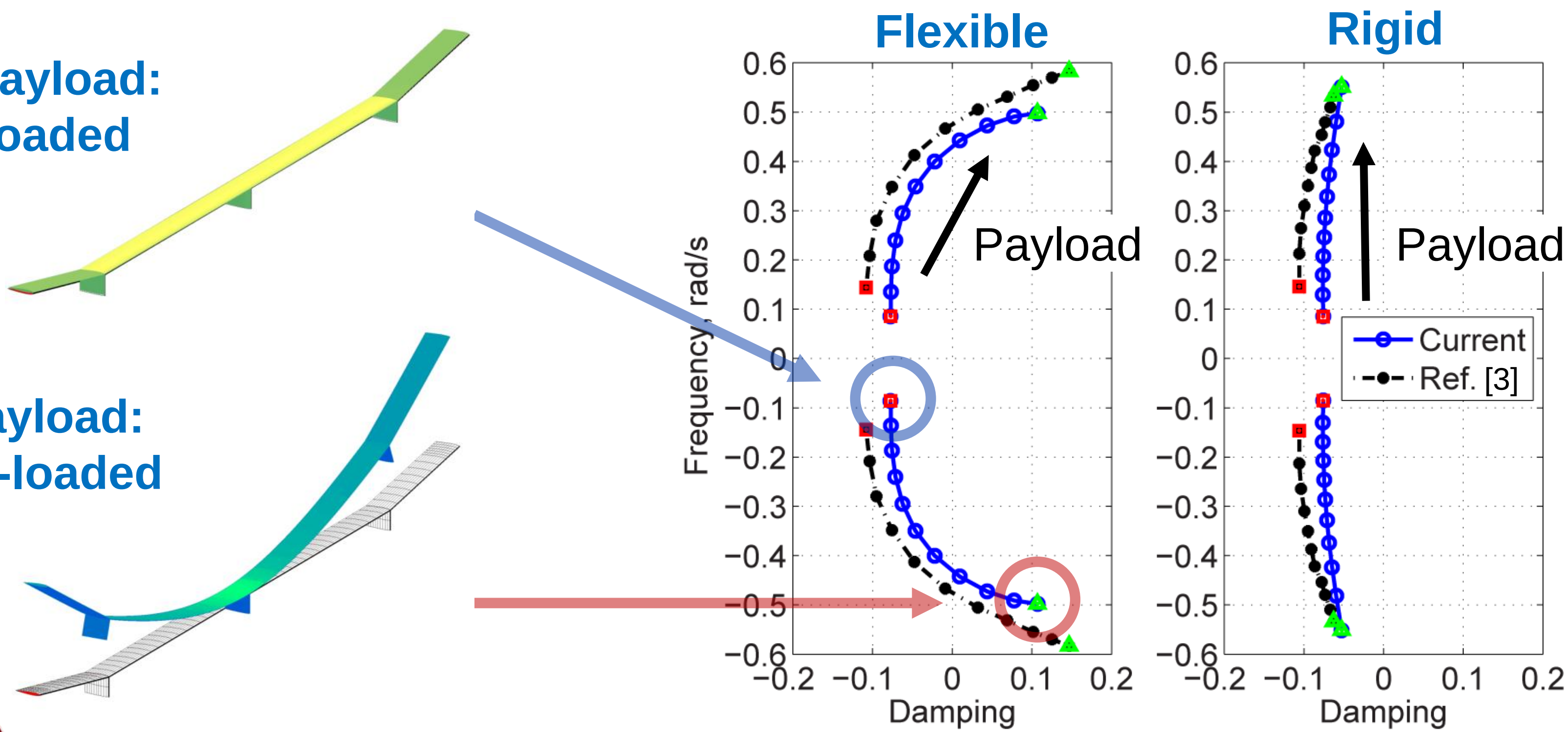

Nonlinear aeroelastic/flight dynamic characteristics dependent on trim conditions

Discrete Non-uniform Gust Model

- Fixed region in space
- Amplitude distribution
  - Peak at center and zero at boundary
  - Possibly different distribution in East and North directions
  - Smooth transition

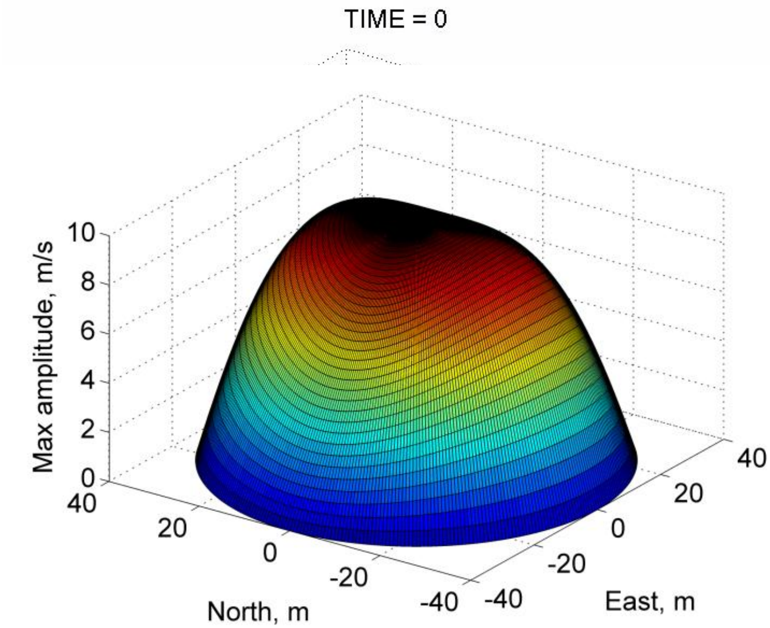

$$A(r,\eta,t)=\frac{1}{2}A_c\left[1-\cos\left(2\pi\frac{t}{t_g}\right)\right]\sqrt{\left(A_E\cos\eta\right)^2+\left(A_N\sin\eta\right)^2}$$

$$A_E(r)=\sin\left(\frac{\pi}{2}\left[1-\left(\frac{r}{r_0}\right)^{n_E}\right]\right)\quad,\quad A_N(r)=\sin\left(\frac{\pi}{2}\left[1-\left(\frac{r}{r_0}\right)^{n_N}\right]\right)\quad,\quad 0<r\le r_0$$

- Time variation: 1-cosine with different temporal durations

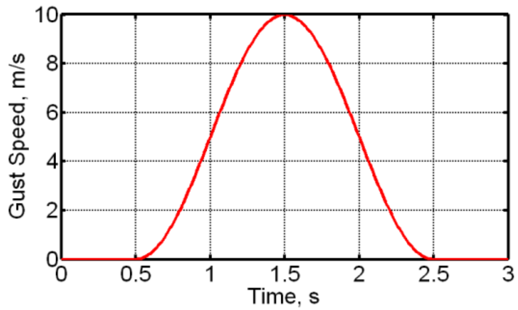

Non-symmetric Gust Input and Response – Fully-Loaded Configuration

- Payload: 227 kg; gust region radius: 40 m; maximum gust center amplitude: 10 m/s
- Non-symmetric gust distribution: gusts mainly applied on right wing

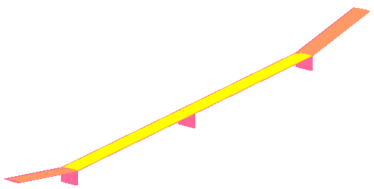

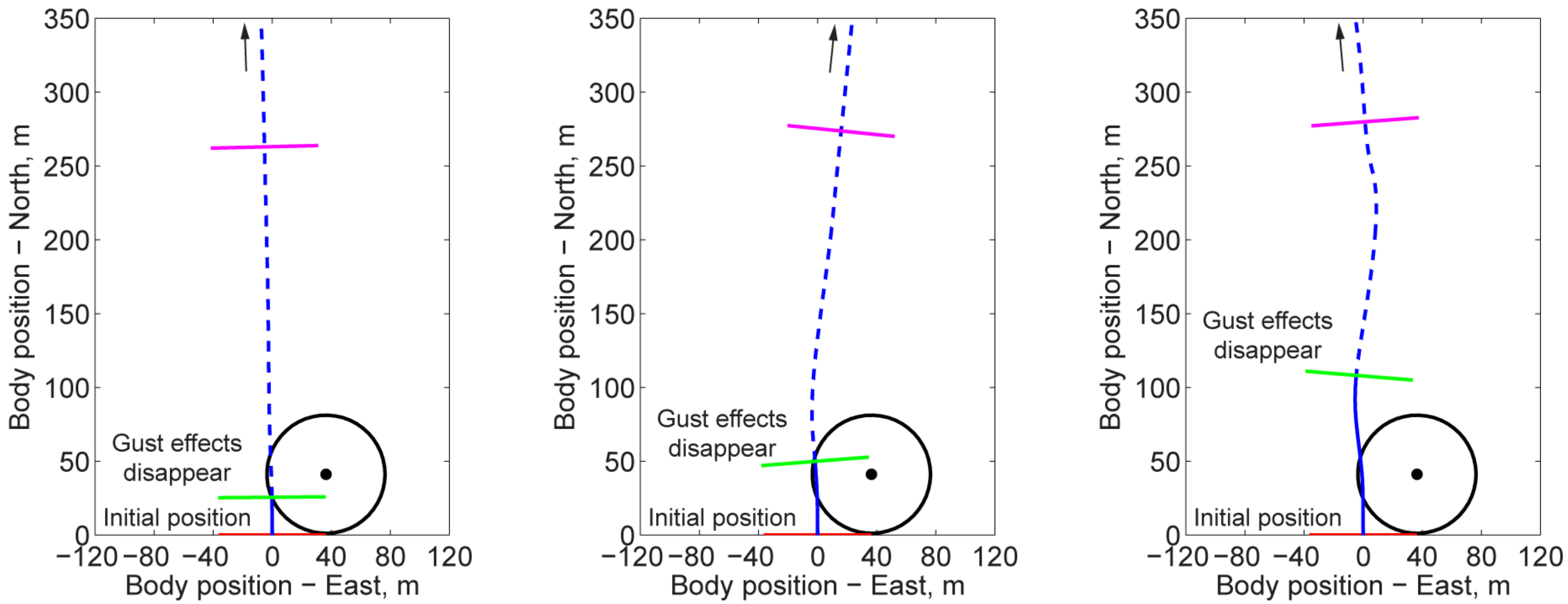

2 s gust duration **4 s gust duration** **8 s gust duration**

Gust duration impacts after-gust flight path

Instantaneous Vehicle Positions and Orientations

- Positions and orientations at 0, 5, 12, 18, 24, and 30 s, respectively

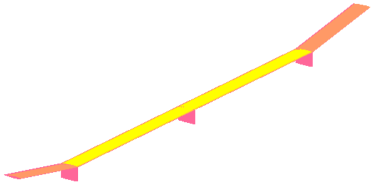

Flight Direction

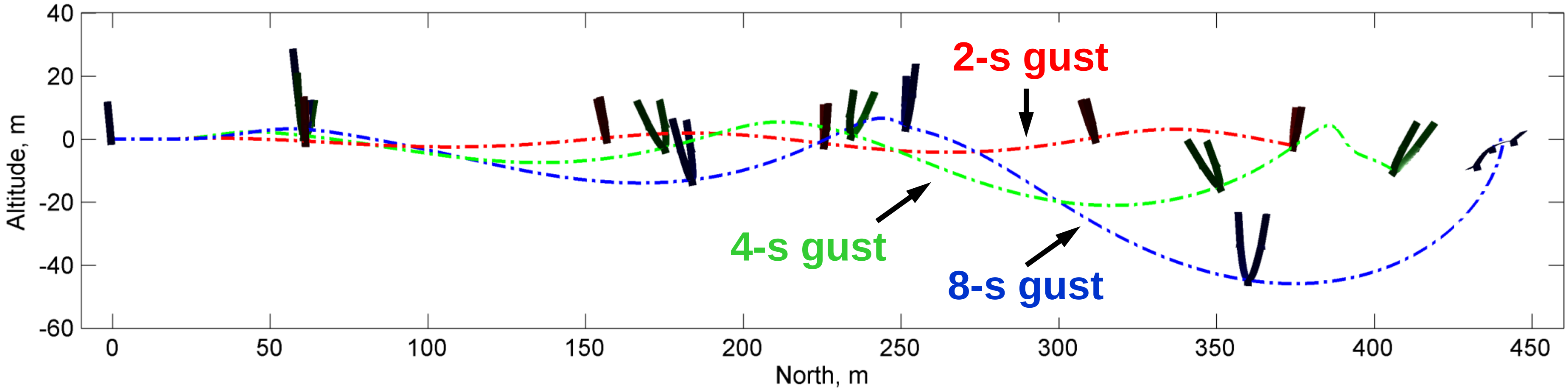

Illustration of unstable Phugoid mode

Animation of Vehicle Motion with Gust Perturbations

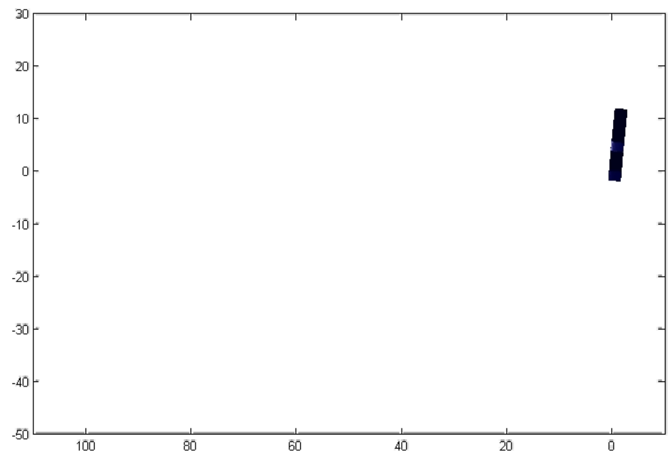

TIME = 0

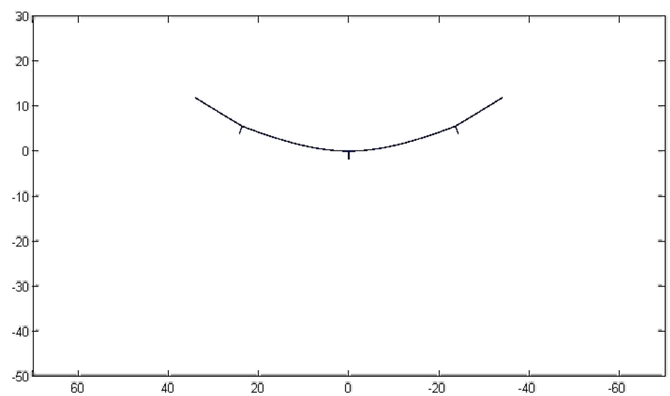

TIME = 0

2-s gust
4-s gust
8-s gust

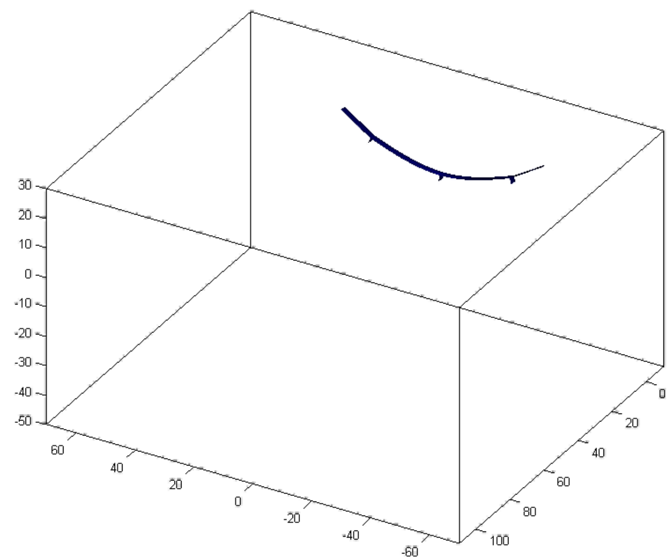

TIME = 0

Experimental Studies

Duke University's Wind-Tunnel Test

- Tang and Dowell's high-aspect-ratio wing with a tip slender body
- Nonlinear aeroelastic tests, studying geometrically nonlinear effects on wing response
- Data available in public domain for code validations

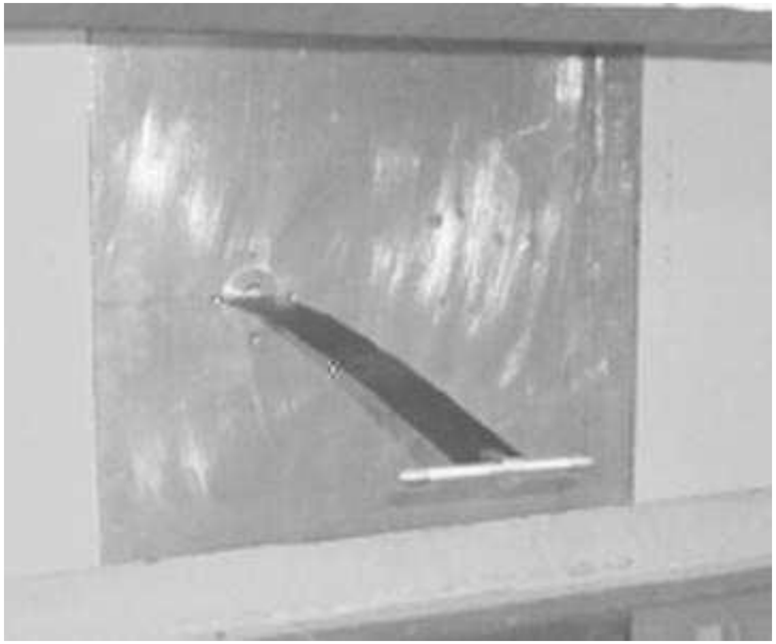

Photo from Tang and Dowell, Duke University

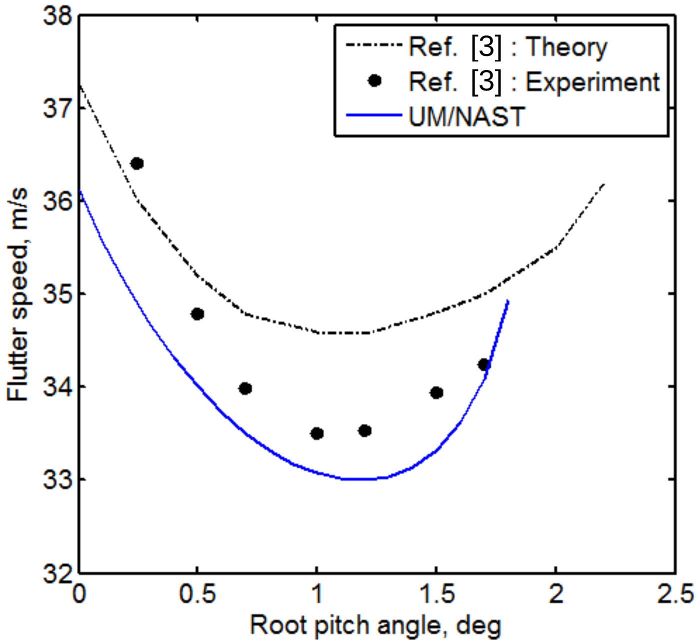

Su, Zhang, and Cesnik, IFASD 2009

No complete vehicle aeroelastic/flight dynamic data available to support full formulation validation

X-HALE Project

- Designed and manufactured in Umich, with support from AFIT and AFRL

My previous institute

- Design, build, and test experimental platform to provide controlled nonlinear aeroelastic / flight dynamic coupled data to be used for code validation

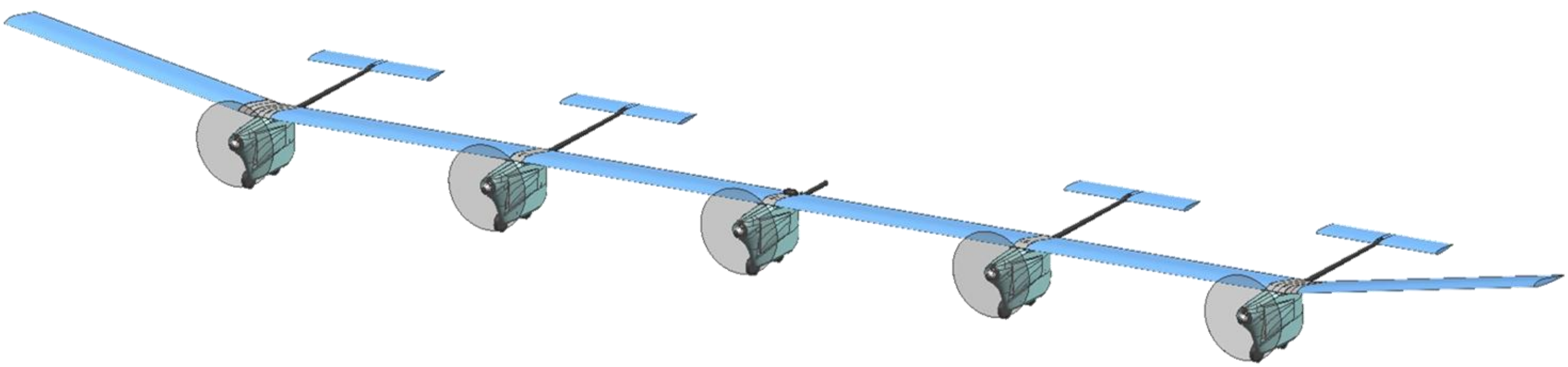

X-HALE Concept

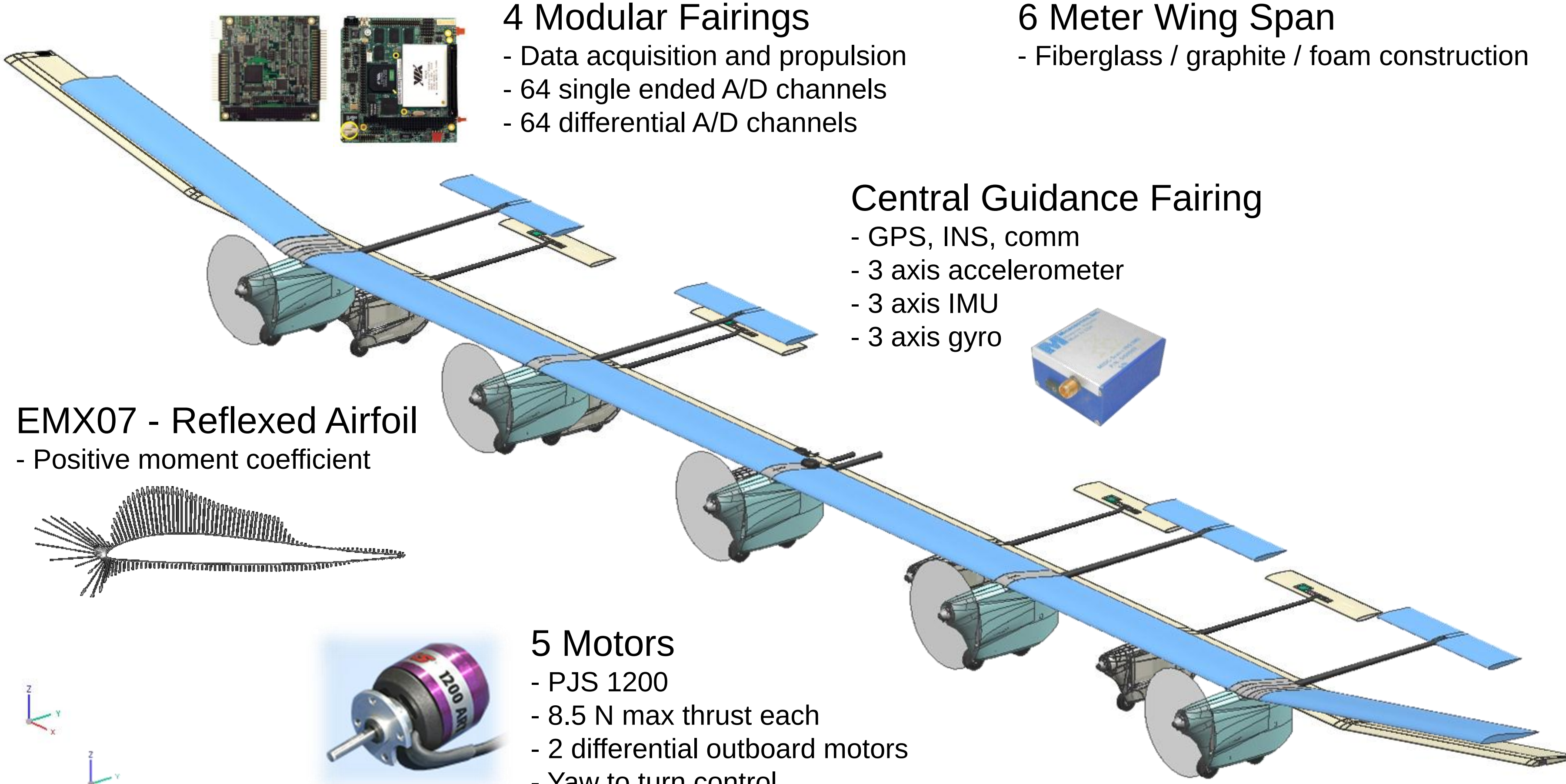

4 Modular Fairings
- Data acquisition and propulsion
- 64 single ended A/D channels
- 64 differential A/D channels

6 Meter Wing Span
- Fiberglass / graphite / foam construction

Central Guidance Fairing
- GPS, INS, comm
- 3 axis accelerometer
- 3 axis IMU
- 3 axis gyro

EMX07 - Reflexed Airfoil
- Positive moment coefficient

5 Motors
- PJS 1200
- 8.5 N max thrust each
- 2 differential outboard motors
- Yaw to turn control

Basic Dimensions

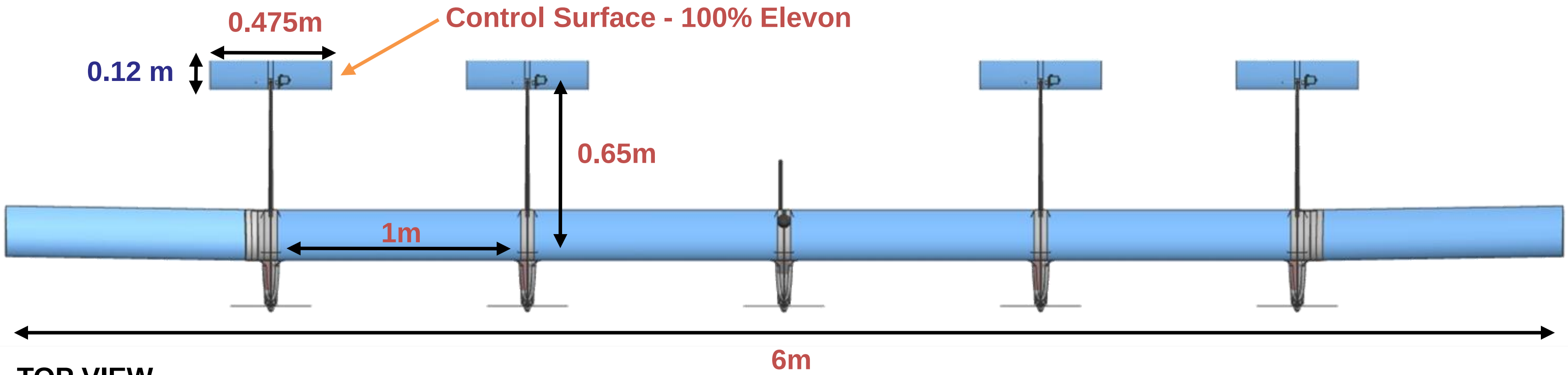

TOP VIEW

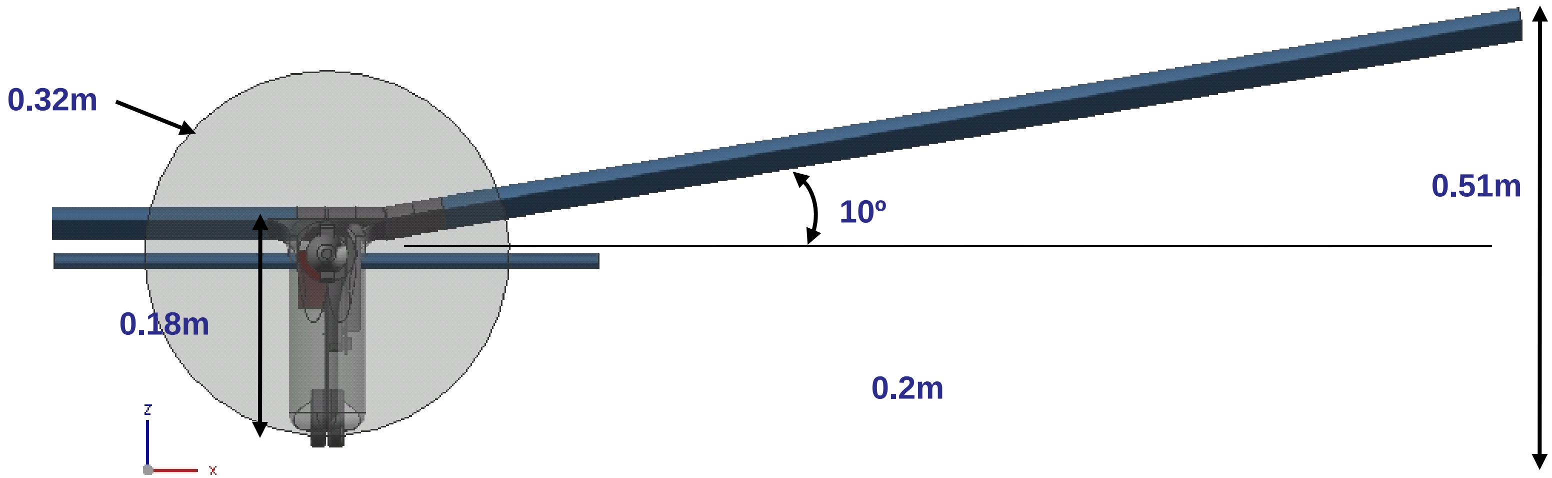

FRONT VIEW CROPPED - WINGTIP

Primary Flight Controls

- Forward thrust – all motors
- Yaw to turn – differential outboard motors
- Pitch – Tails 1 and 2
- Roll – All differential or 2-4 and 1-3 combination
- Ailerons on dihedral wing members

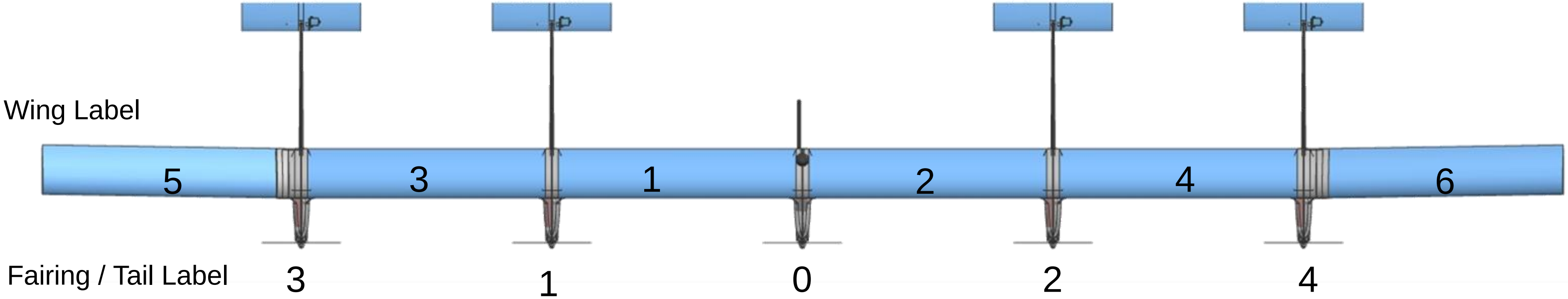

Mixing channels before and after servo switched controller (SSC)

Wing Manufacturing

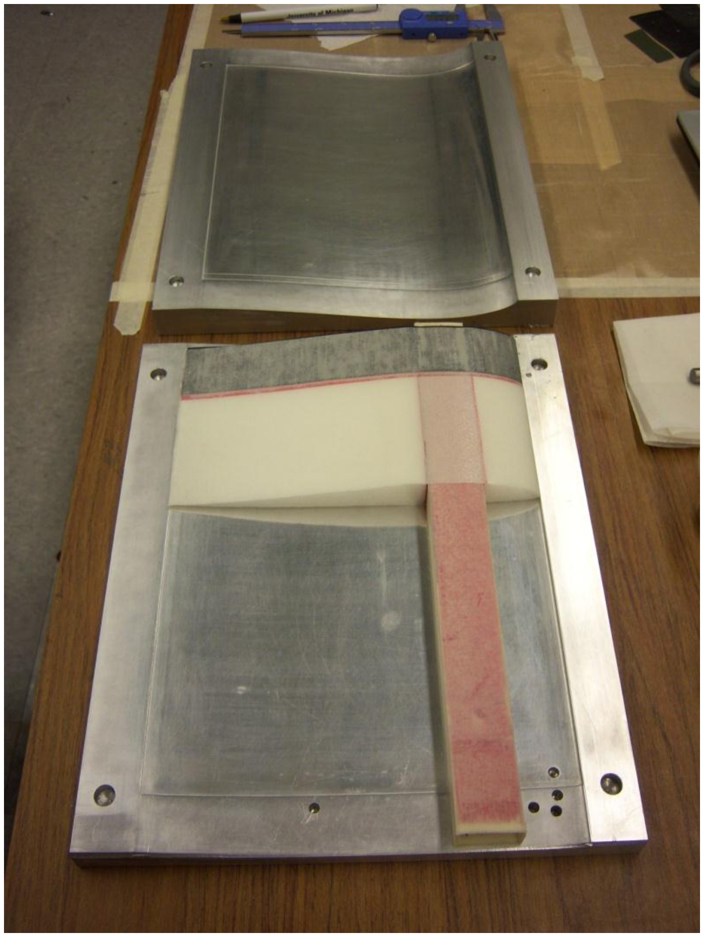

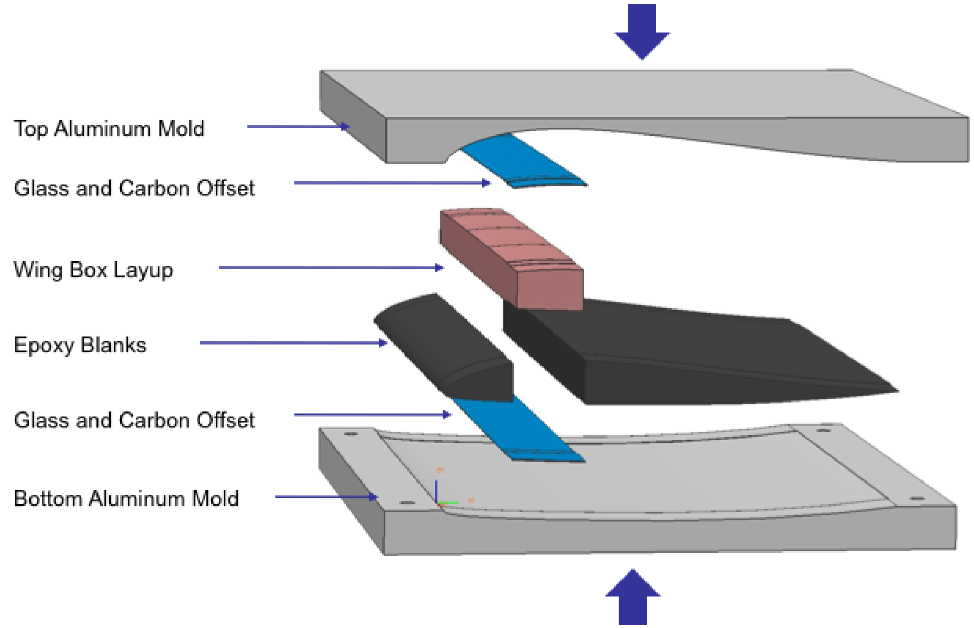

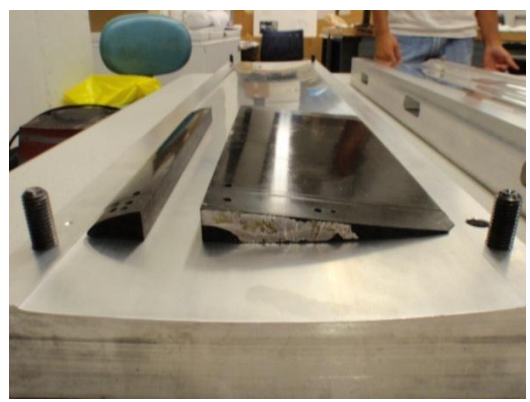

Still Going On…

- Details about X-HALE design/simulation is published[4]
- First "hobby" flight
  - Jan 2011 at UM Oosterbaan Fieldhouse



- First flight of X-HALE
  - Aug, 2012 at Camp Atterbury, IN
- More information to be released in the future

[4] Cesnik, C.E.S., Senatore, P.J., Su, W., Atkins, E.M., and Shearer, C.M., "X-HALE: A Very Flexible UAV for Nonlinear Aeroelastic Tests," *AIAA Journal*, Vol. 50, No. 12, 2012, pp. 2820–2833.

Concluding Remarks

- Numerical framework for modeling and analyzing very flexible aircraft (VFA)
  - Coupled nonlinear aeroelastic/flight dynamic simulation (open and closed loop)
  - Strain-based geometrically-nonlinear beam model
  - Incompressible unsteady aerodynamics (with compressibility corrections and stall models)
  - Rigid-body flight dynamics
  - Non-symmetric, spatially-distributed, discrete gust model
  - Skin wrinkling effects modeled as bilinear torsional stiffness

Concluding Remarks (Cont'd)

- VFA have radically different behavior than conventional aircraft
  - Coupling between aircraft deformation and rigid-body motions changes flutter boundaries
  - Flutter boundary in free flight condition may not be impacted by wing in-plane bending stiffness
  - Finite amplitude gust can excite instabilities
  - High instantaneous angle of attack on some wing stations results in stall, resulting in different transient responses of the wing and may alter the vehicle flight behavior

Concluding Remarks (Cont'd)

- What did we learn from the physics of VFA?
  - Deformed aircraft geometry, which depends on the operating (trim) condition, should be the basis in weight, structural, and stability analyses
  - Traditional linear solution to VFA aeroelasticity might not be sufficient – Nonlinear solution is required
  - Coupling between aeroelasticity and flight dynamics needs to be considered
  - Aeroelastic models should incorporate the rigid-body motion, and vice versa. Individual solutions might not be appropriate

Research on different aspects of Very Flexible Aircraft & Structures are on-going at the University of Alabama!

Ongoing and Future Research Areas

Classic Aeroelasticity

- Aeroelasticity of large-scale very flexible aircraft
  - Next-generation HALE UAVs
    - DARPA, Air Force, Boeing, NASA ……
  - Enhanced structural modeling capability
  - Aerodynamics for different flight conditions and aircraft configurations

USAF X-56A

  - Other emerging technologies in aerospace structures
  - Efficient aeroelastic solutions: real-time flight simulation

Active and Adaptive Aerospace Structures

- Flight is flexible in nature
- Flight is also adaptive in nature
  - Morphing aircraft
- Wing warping (twist and camber)
  - Adaptive structures (ribs)
  - Integrated strain actuation
  - Actuator/sensor/power
  - Control algorithm/mechanism
- Applications – active aeroelastic tailoring and control:
  - Trajectory control
  - Gust/Disturbance alleviation
  - Helicopter vibration/noise reduction
  - etc.

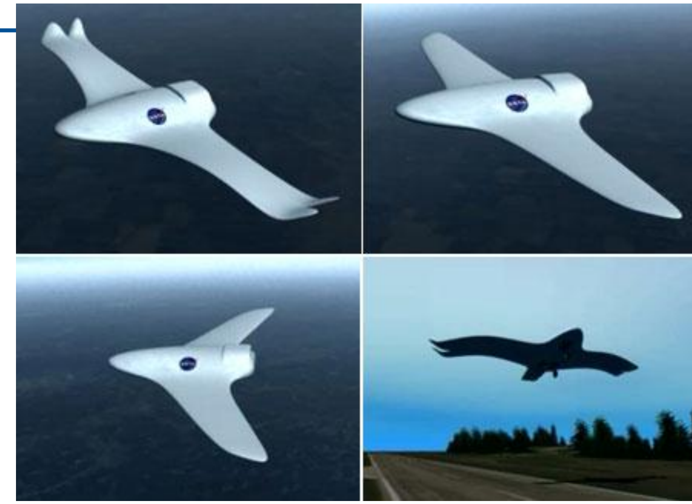

Morphing aircraft concept, NASA Langley

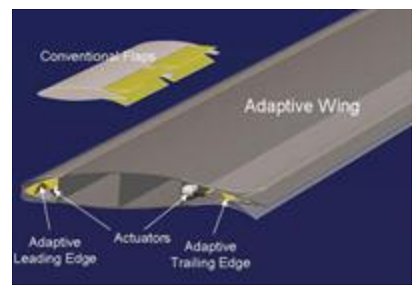

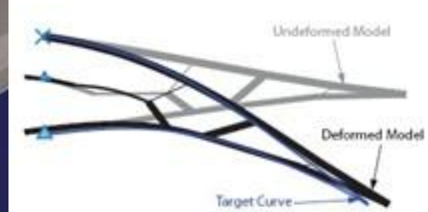

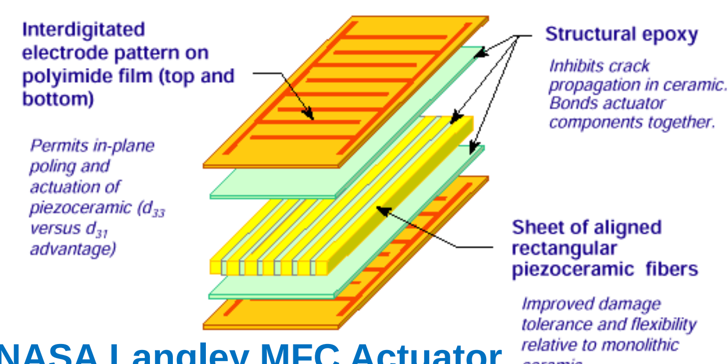

NASA Langley MFC Actuator

(Energy) Self-Sustained Autonomous System

Components of Multidisciplinary Multifunctional Aeroservoelastic Framework

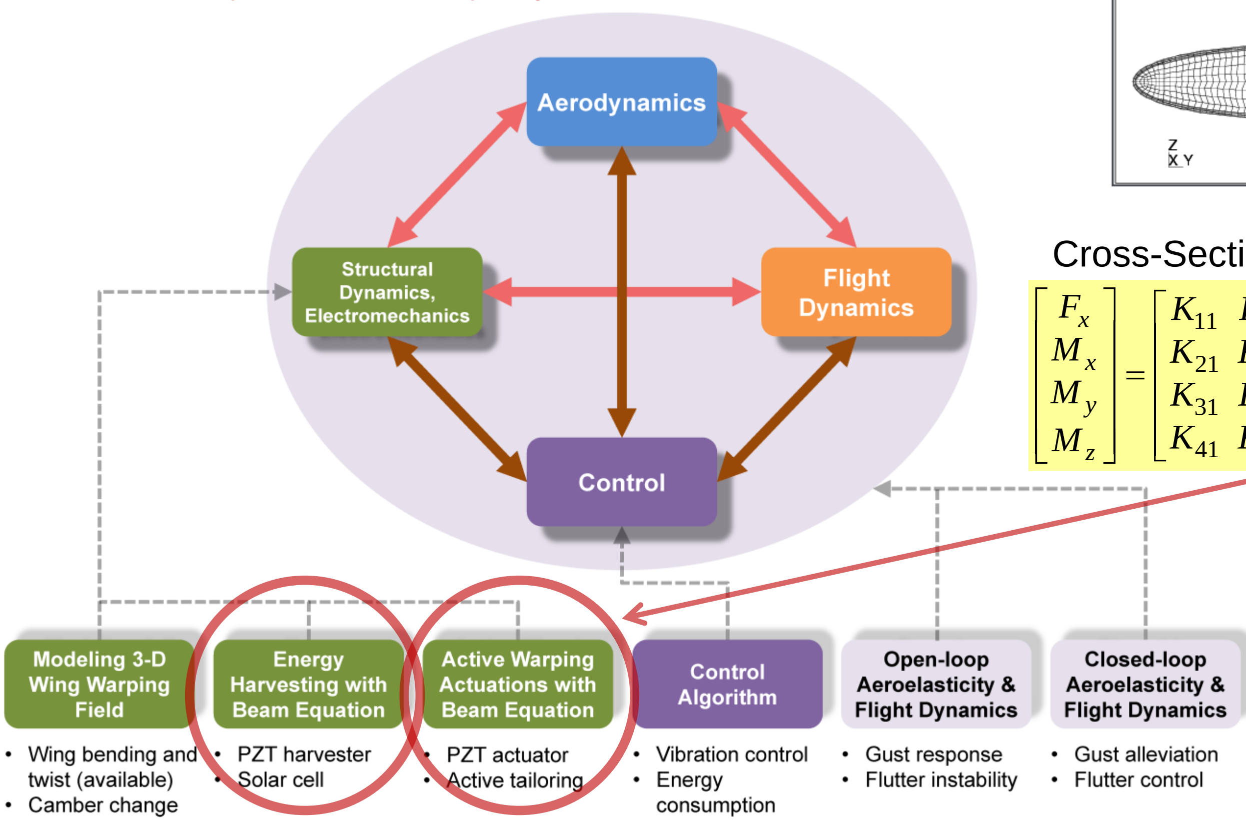

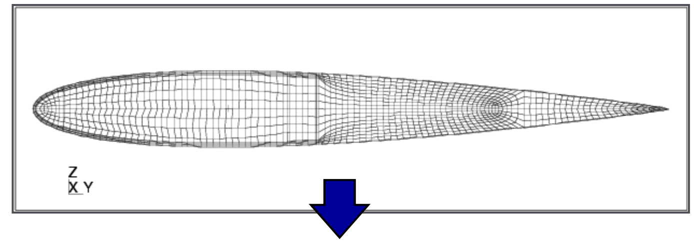

Cross-Section Stiffness and Actuation Constants

$$\begin{bmatrix} F_x \\ M_x \\ M_y \\ M_z \end{bmatrix} = \begin{bmatrix} K_{11} & K_{12} & K_{13} & K_{14} \\ K_{21} & K_{22} & K_{23} & K_{24} \\ K_{31} & K_{32} & K_{33} & K_{34} \\ K_{41} & K_{42} & K_{43} & K_{44} \end{bmatrix} \begin{bmatrix} \varepsilon_x \\ \kappa_x \\ \kappa_y \\ \kappa_z \end{bmatrix} - \begin{bmatrix} B_{11} & B_{12} & \cdots & B_{1m} \\ B_{21} & B_{22} & \cdots & B_{2m} \\ B_{31} & B_{32} & \cdots & B_{3m} \\ B_{41} & B_{42} & \cdots & B_{4m} \end{bmatrix} \begin{bmatrix} v_1 \\ v_2 \\ \vdots \\ v_m \end{bmatrix}$$

Use of piezoelectric effects in two ways

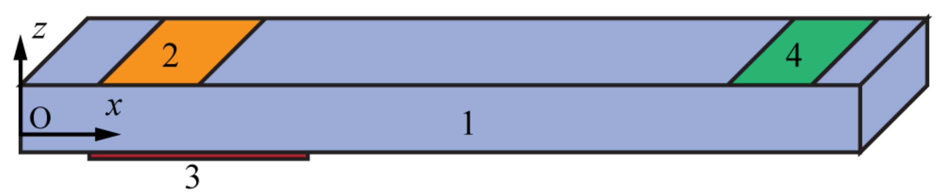

1: Wing spar; 2: PZT harvester;
3: PZT actuator; 4: PCB board.

Rotary Systems – Helicopters and Wind Turbines

- Blade vortex interaction (BVI)
- (Helicopter) vibration, noise
- (Wind-turbine) power generation, fatigue

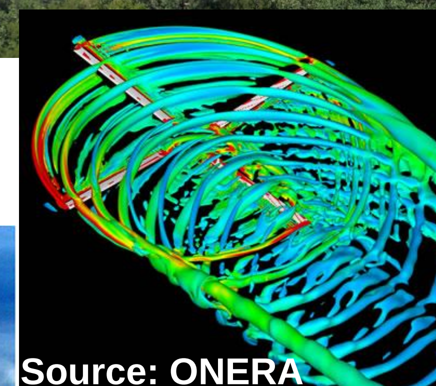

- Active and smart blades
  - Active vibration control
  - Noise reduction
  - Health monitoring

Active Aeroelasticity for Wind Turbines

- Large wind turbines
  - More power generation
  - Flexible blades
- Aeroelastic / acoustic issues
  - Operation speed close to flutter
  - Noise places limit on blade size
- Smart blade
  - Active aeroelastic tailoring for load and flow control
  - Alleviation of disastrous wind load
  - Onboard health monitoring
- What can we model?
  - Nonlinear beam model
  - Active composite materials
  - Need a proper aerodynamic model
  - Experimental support

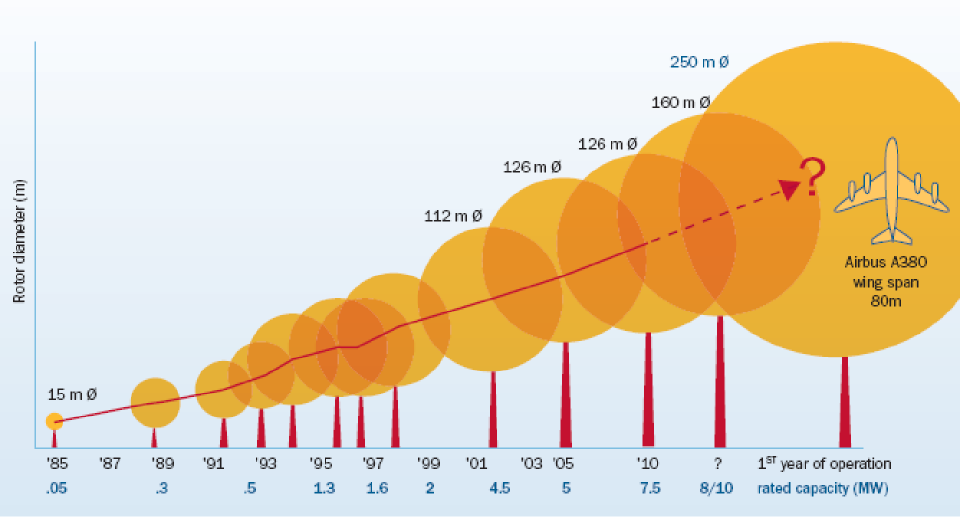

Questions?